Development of an integrated Municipal Solid Waste conversion and CO_2 utilization process for the environmentally friendly production of transportation fuels

Golnoosh Malekiardebili

A Thesis

in

the Department

of

Chemical and Materials Engineering

Presented in Partial Fulfillment of the Requirements

For the Degree of Master of Applied Science at

Concordia University

Montreal, Quebec, Canada

August 2025

CONCORDIA UNIVERSITY

School of Graduate Studies

This is to certify that the thesis prepared

By: Golnoosh Malekiardebili

Entitled: Development of an integrated Municipal Solid Waste conversion and CO_2 utilization process for the environmentally friendly production of transportation fuels

and submitted in partial fulfilment of the requirements for the degree of

Master of Applied Science (Chemical and Materials Engineering)

complied with the regulations of the University and meets the accepted standards with respect to originality and quality.

Signed by the final Examining Committee:

Chair Dr. Nhat Truong Nguye

Examiner Dr. Melanie Jane Hazlett

Supervisor Dr. Yaser Khojasteh-Salkuyeh

Approved by

Date of defense August 27th, 2025

Abstract

Development of an integrated Municipal Solid Waste conversion and CO_2 utilization process for the environmentally friendly production of transportation fuels

Golnoosh Malekiardebili

The global rise in municipal solid waste (MSW) generation and the urgent need to decarbonize the transportation sector, particularly the aviation fuels and heavy trucks, have created a compelling opportunity for circular carbon technologies. This thesis presents the development and analysis of a waste-to-jet fuel production pathway that integrates MSW gasification, syngas conditioning, reverse water gas shift (RWGS) conversion, Fischer-Tropsch (FT) synthesis, and hydrocracking. The process design and simulation are performed using Aspen Plus, with a particular emphasis product selectivity and CO_2 utilization.

Using the simulation results, a comprehensive techno-economic analysis (TEA) is carried out to estimate capital and operating expenditures, minimum selling prices, and project viability under Quebec's low-carbon electricity conditions. Additionally, a detailed life cycle assessment (LCA) is conducted in OpenLCA to evaluate the environmental footprint of the proposed system compared to conventional pathway of jet fuel production and waste incineration. The LCA results, based on ReCiPe methodology, indicate that the MSW-to-jet fuel pathway can achieve net-negative greenhouse gas emissions under low-carbon electricity scenarios.

The findings highlight the dual benefit of MSW valorization: reducing landfill dependency and enabling the production of sustainable aviation fuel (SAF) with a significantly lower carbon intensity. This research demonstrates that MSW can serve as a viable feedstock for decarbonized fuel production, offering a scalable and economically competitive solution aligned with global climate and waste management goals.

Acknowledgments

I would like to express my heartfelt gratitude to my supervisor, Professor Yaser Khojasteh-Salkuyeh, for his continuous support, valuable feedback, and expert guidance throughout the course of this thesis. His insight and encouragement were instrumental at every stage of this research, and I am truly grateful for the opportunity to work under his supervision.

I would also like to extend my sincere thanks to the Natural Resources Canada (NRCan) team for their helpful input and thoughtful feedback on my results, which enriched the quality of this work.

Special thanks go to the members of the CSTAR team for their constructive comments, support, and collaborative spirit during our discussions, which helped me refine various aspects of my research.

I am deeply thankful to my family—my mother, father, and sister—for their unconditional love, encouragement, and belief in me throughout this journey. Their constant support has been my greatest source of strength.

Lastly, I would like to thank my friends for their motivation, patience, and understanding during both the challenging and rewarding moments of this project.

Table of Contents

List of figures vii

List of tables viii

Chapter 1- Introduction 1

1.1. Background and Motivation 1

1.2. Research Objectives 2

1.3. Thesis layout 3

Chapter 2- Literature Review 4

2.1. Municipal Solid Waste: Composition, Challenges, and Environmental Impacts 4

2.2. Waste-to-Energy: Incineration and Its Limitations 5

2.3. Valorization Technologies for MSW 5

2.3.1. Conversion to Chemicals 6

2.3.2. Conversion to Fuels 6

2.4. Gap in Research: Jet Fuel from MSW via FT Synthesis 10

Chapter 3- Process Description 11

3.1. Municipal solid waste feedstock 13

3.2. Gasification Unit 14

3.3. Gas Treatment Unit 16

3.3.1 Scrubbing Section 16

3.3.2. COS Hydrolysis 16

3.3.3. Acid Gas Removal (Amine System – DGA) 16

3.4. Reverse Water Gas Shift (RWGS) Unit 19

3.5. Fischer–Tropsch (FT) Synthesis Unit 21

3.5.1. FT reaction 21

3.5.2. Hydrocracking 25

Chapter 4- Results 28

4.1. Process simulation results 28

4.2. Life cycle assessment 30

4.1.1. Goal and scope definition 30

4.1.2. Life cycle inventory analysis 31

4.1.3. Life cycle impact assessment (LCIA) 33

4.1.4. LCA results 34
4.2. Economic analysis 47
4.2.1. Assumptions 48
4.2.2. Capital Cost Estimation 50
4.2.3. Operating Cost 51
4.2.4. Revenue Estimation 52
4.2.6. NPV and MSP 53
4.2.7. Sensitivity Analysis on MSP 54
Chapter 5- Conclusion 57
Supplementary data 60
A. LCA Results 60
A.1. Comparison of global warming categories in endpoint results 60
A.2. Contribution of co-product on endpoint results 61
References 64

List of figures

Figure 1. Simplified schematic of MSW drying and gasification for chemical and fuel production 1
Figure 2. BFD of the process 11
Figure 3. Solid waste diversion and disposal per person, Canada, 2002 to 2018 [29] 13
Figure 4. Gasification unit 15
Figure 5. Acid gas removal unit 18
Figure 6. RWGS unit 21
Figure 7. Process flow diagram of FT and Hydrocracking sections of the FT unit. 24
Figure 8. Purge gas oxyfuel combustion and CO_2 liquefaction sections. 26
Figure 9. Fractionation section of the FT unit. 27
Figure 10. System boundary for LCA study 30
Figure 11. Comparison of percentage reduction in top 3 impactful midpoint categories 37
Figure 12. Comparison of Top Six Midpoint Impact Categories by Contribution – Conventional vs. MSW-to-Jet Fuel vs. MSW-to-Jet Fuel with Energy Allocation 38
Figure 13. Percentage of improvement in MSW-jet fuel vs. incineration 39
Figure 14. Relative Midpoint Impact Improvements of MSW-to-Jet Fuel, Soybean, and Palm Pathways Compared to Waste Cooking Oil 42
Figure 15. Percentage improvement in human health-related endpoint impact categories for the MSW-to-jet fuel process relative to conventional jet fuel production 45
Figure 16. Percentage improvement in ecosystem quality–related endpoint impact categories for the MSW-to-jet fuel process relative to conventional jet fuel production 46
Figure 17. Percentage improvement in resource quality–related endpoint impact categories for the MSW-to-jet fuel process relative to conventional jet fuel production 47
Figure 18. Impact of Electricity and MSW Price Variations on MSP 54
Figure 19. Sensitivity analysis of key financial parameters on the minimum selling price of jet fuel 55
Figure 20. Relative Impact Comparison for Global Warming Categories (Project vs. Conventional Pathway) 60
Figure 21. Comparison of the base case LCA results with scenarios excluding individual co-products 62

List of tables

Table 1. Overview of Biomass-Based Jet Fuel LCA Studies and Key Findings 10
Table 2. Main process design parameters of each unit 12
Table 3. MSW data and composition 14
Table 4. Some parameters of the raw syngas stream 15
Table 5. Equilibrium Reactions and Constants for DGA-Based Acid Gas Absorption in the Absorber Column 18
Table 6. Mass fraction of impurities before and after treatment 19
Table 7. Some parameters of the clean syngas 19
Table 8. Mass fraction of main components before and after RWGS 21
Table 9. Design parameters of the FT reactor 24
Table 10. Summary of simulation results 28
Table 11. Electricity consumption of each process unit 29
Table 12. Summary of energy efficiency 29
Table 13. LCI inputs and outputs 33
Table 14. Midpoint assessment to produce 1kg of jet fuel in this project from MSW vs. conventional pathway vs. MSW-to-jet fuel with energy allocation 36
Table 15. Midpoint assessment to produce MJ of jet fuel and electricity from 1kg of MSW 39
Table 16. Comparison of midpoint life cycle impact category results for the MSW-to-jet fuel pathway and selected bio jet fuel pathways from the literature 41
Table 17. Endpoint categories to produce 1 kg of jet fuel in the project vs. the conventional pathway 44
Table 18. Economic analysis parameters, assumptions, and prices 48
Table 19. Summary of unit cost and CAPEX 51
Table 20. Summary of OPEX 52
Table 21. Summary of feedstock cost and total revenue 52
Table 22. Base Case and Contribution of Individual Co-Products to Selected Endpoint Impact Categories 61

Chapter 1- Introduction

1.1. Background and Motivation

Immense environmental challenges have been created due to the growth of the population and economic development [1]. Generation of a large amount of municipal solid waste (MSW) is one of these challenges, which is expected to increase [2]. It has been studied that the amount of globally produced MSW will reach around 2.2 billion tons per year by 2025 [3]. Therefore, an increase in waste generation is inevitable, and scientists are trying to develop effective processes for reducing the negative impacts of waste on the environment and human health [4]. Landfills are still the major technique of disposing of waste because of several reasons, including low cost and simplicity [4]. However, there will be negative impacts on the environment with greenhouse gas emissions, and also on human health due to pollution of resources like water and soil [3]. Furthermore, the circular economy is also impacted negatively by landfilling, and to overcome that, value should be added to waste via different processes [2]. Nowadays, waste-to-energy is one of those processes. With incineration, not only is energy produced, but also the weight and volume of waste are reduced significantly [3]. The main drawback of incinerating waste is the flue gas formation, resulting in air pollution and lowering the system efficiency due to corrosion issues [5]. Compared to incineration, gasification has lower emissions and, all in all, is more efficient and cleaner [6]. Through gasification, most of the organic content of MSW is converted to syngas, which can be further converted to fuel [5]. For the reasons mentioned, waste-to-energy through gasification coupled with carbon capture is believed to be an effective way of reducing waste and simultaneously producing energy and fuel, making the world less dependent on fossil fuels [7]. From another point of view, the high-water content of MSW would be challenging for processes, as it would lower the efficiency and increase the cost of the plant. So, prior to gasification, a drying unit is necessary to mitigate these challenges [3]. Figure 1 shows the whole idea of this project and how it deals with the design of an efficient process that incorporates MSW drying and conversion to syngas process for reducing the load on the hydrogen unit of CCU processes.

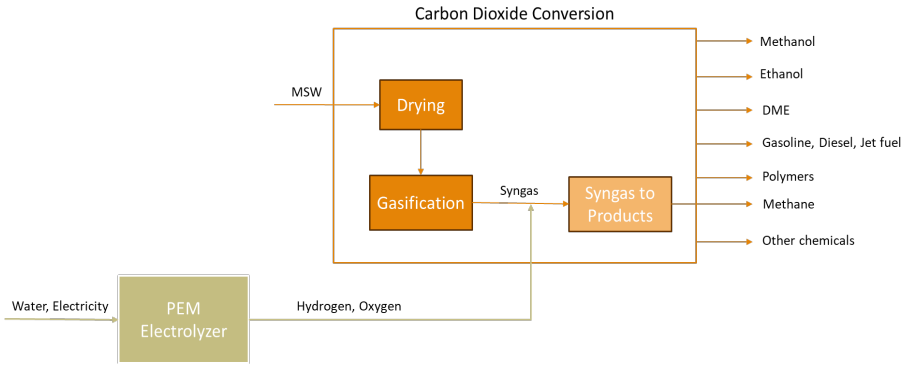

Figure 1. Simplified schematic of MSW drying and gasification for chemical and fuel production

In this work, we developed an integrated process for the co-conversion of MSW and CO_2 into transportation fuel with the focus on jet fuel and diesel. The dried MSW is used as the feed of the gasification unit to produce high-quality syngas with minimum GHG emissions [8]. To clean the impurities and convert the excess CO_2 into CO, the syngas is then passed through treatment and reverse water-gas shift units, respectively. The clean syngas from both routes are mixed and sent to the conversion unit to produce transporation fuels such as diesel and jet fuel.

Air transport is an imminent part of these modern days, which is considered one of the main contributors to GHG emissions. The International Air Transport Association (IATA) is looking to have around 30% of the jet fuel usage replaced by bio jet fuel by 2030 [9]. For this reason, jet fuel is chosen as the desired product in this project. In order to turn our syngas into jet fuel, Fischer-Tropsch (FT) synthesis is used, during which carbon-based materials are converted into an oil product. This product can then be refined to chemical or petrochemical products, which in this case is mainly jet fuel [10]. After simulation of the mentioned process units (drying, gasification, treatment, reverse water gas shift, and Fischer-Tropsch) in Aspen Plus, a life cycle assessment (LCA) study will be carried out on the project, enabling the comparison of emissions and impacts on the environment in conventional and non-conventional (from MSW) jet fuel. Also, techno-economic analysis will be examined by the end of this project.

1.2. Research Objectives

The primary objective of this research is to design a sustainable waste-to-jet-fuel (WTJF) production pathway with minimum greenhouse gas emissions. The study involves the conceptualization, design, and simulation of a complete thermochemical process chain in Aspen Plus®, consisting of drying, gasification, syngas cleaning and treatment, Reverse Water Gas Shift (RWGS) reaction, FT synthesis, hydrocracking, and final fractionation using a PetroFrac column.

This investigation proceeds through the following key stages:

1. Using Aspen Plus® (v14) to model and simulate processes to find mass and energy balances, carbon conversion efficiency, and product distribution.
2. Using the Aspen Process Economic Analyzer (APEA) to do a techno-economic analysis of jet fuel, looking at its capital expenditure (CAPEX), operating expenditure (OPEX), annual income, net present value (NPV), and minimum selling price (MSP).
3. A sensitivity study of important economic factors, such as the price of electricity.
4. Life Cycle Assessment (LCA) using OpenLCA (v1.11), which looks at the environmental effects of different functional units (like 1 kg of jet fuel and 1 MJ of jet fuel) at both the midpoint and endpoint levels. This is compared to normal jet fuel and incineration scenarios.

The aim is to find out if making jet fuel from MSW is a good idea for the environment, for energy efficiency, and for the economy. The main goal is to make this pathway a scalable, low-carbon solution that fits with climate change goals for 2030 and 2050 around the world.

1.3. Thesis layout

Chapter 2 provides a thorough assessment of the literature on MSW as a feedstock, covering its composition, availability, and ways to make it more valuable. It shows how MSW can be turned into fuels and chemicals, and it compares the several ways that waste may be used to make jet fuel.

Chapter 3 talks about the design of the process and the way it was simulated in this study. It starts with the properties and processing of MSW, then goes into detail into each unit operation: gasification, syngas cleaning and treatment (which includes scrubbing, COS hydrolysis, and acid gas removal), the RWGS unit, and the Fischer-Tropsch synthesis unit. The next parts talk about the hydrocracking unit and the distillation column that separates the final products into naphtha, kerosene (jet fuel), diesel, and light ends.

Chapter 4 shows the results of the techno-economic analysis (TEA) and the life cycle assessment (LCA). The LCA part has the goal and scope definition, the life cycle inventory (LCI), the impact assessment (LCIA), and the explanation of the midpoint and endpoint outcomes. There is a separate section that discusses the environmental impacts of Quebec's power mix. The TEA part talks about capital and operational expenses, net energy efficiency, estimating revenue, the minimum selling price (MSP), and the net present value (NPV). There is also a sensitivity study to look at how changes in electricity and MSW prices, and some assumptions regarding the economic analysis, affect the economy.

Lastly, Chapter 5 sums up the main results of this study, makes general conclusions, and suggests ways for further research in the area of turning MSW into jet fuel.

Chapter 2- Literature Review

2.1. Municipal Solid Waste: Composition, Challenges, and Environmental Impacts

Municipal Solid Waste is a mix of waste from homes, businesses, and other places that is thrown away. It usually has biodegradable organic waste (such as food scraps and yard clippings), paper, cardboard, plastics, metals, textiles, and inert materials like ash and dirt. As cities throughout the world grow and people buy more things, the amount of MSW produced around the world is expected to rise. MSW has a big effect on the ecosystem. If not managed properly, MSW can cause a lot of pollution in the air, water, and soil. In low- and middle-income nations, open dumping and unregulated landfilling are still the most common ways to get rid of this waste. In anaerobic landfill settings, the breakdown of organic material generates methane (CH_4), a greenhouse gas (GHG) with a global warming potential (GWP) 28–36 times higher than CO_2 over a century [34].

In recent years, Life Cycle Assessment (LCA) has become a strong way to look at the environmental costs of different ways to deal with MSW. Many studies that use life cycle assessment have looked at how traditional methods like landfilling and incineration compare to newer ones like waste-to-energy (WtE), anaerobic digestion, and thermochemical conversion to fuels or chemicals. Laurent et al. (2014) performed a meta-analysis of more than 200 LCA studies and determined that thermal treatment with energy recovery and biological treatment with biogas capture generally exceed landfilling across various impact categories, including climate change, acidification, and eutrophication. Nonetheless, LCA outcomes are frequently contingent upon context, shaped by geographic location, waste composition, energy mix, and system limitations [11].

Also, people are starting to see MSW not just as a problem to get rid of, but also as a way to get materials and energy back. This change is in line with the concepts of a circular economy and the goals of sustainability. So, precise environmental assessments are essential for directing policy and investment choices in waste management infrastructures.

According to the IPCC 2006 and other LCA studies, unmanaged landfilling, especially in low- and middle-income countries, might release up to 1,000 kg CO_2-eq per tonne, mostly because methane is released without any controls [12].

Landfilling causes a lot of acidification, eutrophication, and freshwater ecotoxicity because it makes leachate and releases heavy metals and pollutant gases. Ouedraogo et al. (2021) say that landfilling can induce acidification up to 1.58 kg SO_2-eq per tonne of MSW, mostly because of sulfur and nitrogen compounds being released into the air. The potential for eutrophication is likewise high, at 0.254 kg PO_4^{3-}-eq per tonne, because leachates that are high in nutrients can pollute nearby bodies of water. Additionally, the possibility of freshwater ecotoxicity, which is related to the leaching of heavy metals and long-lasting organic compounds, is especially worrying for landfills that are getting older or not being managed well. These environmental loads show how much better modern alternatives are, like gasification, which has far lower values in these

areas (for example, 0.10 kg SO_2-eq/t for acidification)[13]. These results show that thermochemical conversion paths like gasification are better for the environment than traditional landfill disposal, especially when used alongside technologies that manage pollution downstream. Anaerobic degradation in landfills follows the simplified reactions:

$$Hydrolysis: C_6H_{10}O_5 + H_2O \rightarrow C_6H_{12}O_6 \quad (1)$$

$$Acidogenesis: C_6H_{12}O_6 \rightarrow 2CH_5CH_2OH + 2CO_2 \quad (2)$$

$$Acetoclastic\ Methanogenesis: CH_3COOH \rightarrow CH_4 + CO_2 \quad (3)$$

$$Hydrogenotrophic\ Methanogenesis: CO_2 + 4H_2 \rightarrow CH_4 + 2H_2O \quad (4)$$

2.2. Waste-to-Energy: Incineration and Its Limitations

One common way to get value from MSW is to burn it to get energy. In places like Japan, Sweden, and Germany, waste-to-energy (WtE) incineration plants are already well-known. They can cut down on the amount of waste by up to 90% and provide power and district heating. But WtE also has certain environmental costs. The IPCC (2006) says that burning 1 tonne of MSW releases about 0.7–1.2 tons of CO_2 [12]. Fossil carbon contribution accounts for around 280–480 kg CO_2-eq per tonne of waste. While modern WtE plants can achieve net energy generation efficiencies of 20–25%, they also produce residual bottom ash, flue gas treatment residues, and pose risks of air pollutant emissions, including dioxins and NOx [14].

A simplified waste combustion reaction follows the equation below:

$$C_xH_yO_z + O_2 \rightarrow CO_2 + H_2O + heat \quad (5)$$

Although energy recovery offers advantages over landfilling, its contribution to climate change, respiratory effects, and terrestrial acidification must be critically examined. LCA-based comparisons (Laurent et al., 2014) consistently show that incineration performs better than landfilling in global warming and fossil resource depletion categories, but underperforms when compared to more advanced thermochemical or biochemical pathways [11].

2.3. Valorization Technologies for MSW

Valorization of MSW, turning waste into useful goods, is becoming an increasingly important part of circular economy models. It has a lot of promise to cut down on the need for landfills, save resources, and lower greenhouse gas (GHG) emissions. The valorization of MSW can be broadly divided into two primary technological pathways: (1) turning it into chemicals and (2) turning it into fuels. Each pathway has its own steps that are based on the properties of MSW. Many studies have looked at how these steps affect the environment and the economy.

2.3.1. Conversion to Chemicals

Thermochemical or biological techniques that break down complex organic materials into simpler molecules are sometimes used to make chemicals from MSW. These smaller compounds can then be turned into various chemicals. Some important examples are making syngas, methanol, ethanol, lactic acid, and other chemicals that the chemical industry needs.

Gasification is a thermochemical process that turns MSW into syngas, which is mostly made up of carbon monoxide (CO) and hydrogen (H_2). A simplified gasification reaction can be seen in Equation 6:

$$C + H_2O + O_2 \rightarrow CO + H_2\ (+CO_2) \quad (6)$$

A catalyst can be used to turn this syngas into compounds like methanol, dimethyl ether (DME), or ammonia. In some works, the advantages of waste gasification are compared to incineration, citing its superior energy efficiency and enhanced capacity for chemical recovery. They showed that gasification might have a GWP that is 15–25% lower and a fossil depletion that is 40% lower than incineration [15].

Fermentation methods are also getting more attention, especially for the part of MSW that can be broken down by bacteria. Food and paper waste are examples of organic materials that can be fermented into ethanol or volatile fatty acids (VFAs).

Anaerobic acidogenic fermentation is a promising way to generate revenue from the organic part of MSW. This process makes VFAs such as acetic, propionic, and butyric acids. A pilot-scale study examining the fermentation of MSW-derived biowaste in mechanical-biological treatment (MBT) facilities indicated optimal yields between 0.49 and 0.59 g COD VFA per g VS at 35 °C, which is roughly equivalent to 0.5 to 0.6 g VFA per g volatile solids. The effluent, which is high in VFA and mostly acetic and propionic acids, can be used to make biodegradable plastics or turned into bio-based solvents [16].

Lactic acid, an important building block for polylactic acid (PLA) bioplastics, has also been made using feedstocks that come from MSW. For instance, Papadopoulou et al. (2023) exhibited effective lactic acid fermentation with hydrolysates derived from candy-industry waste and biogas digestate, attaining final concentrations of approximately 66 g/L and a productivity rate of 1.37 g/(L·h). While our research concentrated on food-industry leftovers, fermentation methodologies may be relevant to the organic fraction of municipal solid waste [17].

2.3.2. Conversion to Fuels

Turning MSW into fuels, both gas and liquid, has become an important part of the switch to renewable energy. This route is especially appealing because it has two benefits: it cuts down on waste and gives us other options besides fossil fuels.

Pyrolysis and gasification can also be used to make syngas, which can then be turned into synthetic natural gas (SNG), methanol, or FT fuels like synthetic diesel and jet fuel. FT synthesis reaction typically follows the equation below:

$$(2n + 1)H_2 + nCO \rightarrow C_nH_{2n+2} + nH_2O \quad (7)$$

Recent improvements in hydrothermal liquefaction (HTL) make it possible to turn wet MSW directly into bio-crude that can be used as a transportation fuel. For instance, Yu et al. (2023) used HTL on food and yard waste fractions. They got biocrude yields of about 10.6 wt% (non-catalytic) and 17.6 wt% with K_2CO_3 catalysis. They also showed that lifecycle GHG emissions were about 50% lower than those of traditional petroleum-derived fuels [18].

Anaerobic digestion is also a frequent way to turn the organic part of MSW into biogas, which is a mix of methane and CO_2. This biogas can be utilized as is or turned into biomethane. According to Scarlat et al. [19] Europe produced more than 10 billion m^3 of biogas per year from MSW and other organic waste. Germany and Italy were the countries that used it the most.

Despite the increased interest in waste valorization, there remains a considerable gap in the literature explicitly addressing the direct conversion of MSW into jet fuel. Some studies have looked at using MSW as a feedstock to make intermediate products like syngas or biocrude, but not many have looked at or modeled the whole process from MSW to finished aviation fuels. Conversely, there exists a more extensive and developed corpus of research pertaining to biomass-derived sustainable aviation fuels (SAFs), especially through the utilization of agricultural and forestry leftovers by gasification, rapid pyrolysis, fermentation, or Fischer–Tropsch synthesis. This difference shows how important this project is, which tries to connect the two fields by looking into whether it is possible to turn MSW directly into aviation fuel. To contextualize this gap and use adjacent research, the subsequent section examines recent literature on jet fuel synthesis from biomass feedstocks. These studies offer significant insights into conversion technologies, life cycle impacts, and process optimization methodologies that can guide and facilitate the development of MSW-to-jet fuel pathways.

Liu and Yang developed a comprehensive well-to-wake life cycle assessment system for drop-in jet fuel produced from diverse agricultural residues, including corn stover, bean stalks, wheat straw, and rice straw, meticulously tracking the full lifecycle from biomass agriculture to fuel burning in aircraft. They looked at conversion strategies that included quick pyrolysis or gasification, followed by upgrading by FT synthesis or the Alcohol to Jet (ATJ) process. Their findings indicate that jet fuel obtained from agricultural residues attains a CO_2 equivalent of merely 17.9 g/MJ, signifying an approximate 80% reduction in comparison to the 90.2 g CO_2 equivalent per MJ of typical fossil jet fuel. A thorough uncertainty and sensitivity analysis demonstrated that assumptions regarding hydrogen and methanol supplies, process efficiency, transportation distance, and land use emissions—especially concerning rice straw—significantly influence the predicted lifecycle greenhouse gas emissions [20].

Pierobon et al. performed a comprehensive life cycle assessment of iso paraffinic kerosene (IPK) derived from slash-pile woody biomass, employing both mass allocation (100% slash recovery) and system expansion methodologies. The global warming potential (GWP) was about 26 kg CO_2 eq/GJ under the mass allocation, 100% recovery scenario. This is a 70% decrease from fossil kerosene. Also, the ecotoxicity effect was much lower, about 47 CTUe/GJ instead of 234 CTUe/GJ for petroleum jet. The acidification potential also went down a little, by roughly 7%. The study shows that not burning slash piles has net negative consequences on cancer and respiratory health. Nonetheless, it identified no enhancement in acidification and eutrophication under certain scenarios, highlighting the significant impact of allocation choice on outcomes [21].

Moreover, Ahire et al. conducted a techno-economic evaluation and a well-to-tank life-cycle analysis of Fischer–Tropsch synthetic paraffinic kerosene (FT SPK) produced from forest residues. Their process model, which is for a facility that can handle 90 Mg/day, includes gasifying woody biomass and converting it to FT using a catalyst. Considering co-product credits, the minimum selling price is projected to be $1.44/L of fuel (or $1.87/kg), and the global warming potential is about 24.6 g CO_2 eq/MJ, which is lower than what has been reported for other lignocellulosic SAF pathways. The study also does a sensitivity analysis on changes in soil carbon to show how different assumptions about land use affect how well carbon is removed. It assesses supply logistics and feedstock preprocessing, emphasizing the significance of optimization in attaining both environmental sustainability and economic viability at scale [22].

Moretti et al. conducted both attributional and consequential life cycle assessments of biojet fuel derived from potato by-products. Their attributional LCA model indicates a reduction of roughly 60% in greenhouse gas emissions relative to traditional jet fuel. Conversely, the consequential LCA reveals a more complex scenario: replacing the feed with locally-sourced European animal feed leads to a 5–40% reduction in emissions, whereas substituting it with imported soybean meal may cause a rise of up to 70%, contingent on land-use assumptions. The two studies differ greatly in how they describe the creation of photochemical ozone, but they both suggest that acidification, terrestrial eutrophication, and fossil fuel resource depletion are all benefited. These results show how different ways of allocating resources and making assumptions about substitutions can have a big effect on LCA results [23].

Han et al. conducted a comprehensive well-to-wake life cycle assessment utilizing the GREET® model to analyze various advanced aviation fuel paths, including hydrotreated renewable jet (HRJ) derived from oilseed feedstocks, Fischer-Tropsch jet (FTJ) from corn stover, and pyrolysis-based jet from corn stover. When employing corn stover, they say that HRJ reduces GHGs by 41–63%, pyrolysis-derived jet reduces them by 68–76%, and FTJ reduces them by up to 89%. Fertilizer and its associated N_2O emissions, as well as the use of hydrogen and natural gas in fuel generation, are two of the main things that add to overall emissions. Sensitivity tests show that the mix of biomass, the methods used to allocate it, the source of H_2, and the manner carbon capture is done can all change the results a lot between paths [24].

Batten et al. examined a bio-based jet fuel pathway that employs corn stover as feedstock, which is transformed by isoprene fermentation, subsequent dimerization, and hydrotreatment to get 1,4-dimethylcyclooctane (DMCO). They used chemical process simulations, a well-to-wake life cycle assessment, and a techno-economic analysis to see how effectively this integrated approach worked. The study found that the greenhouse gas intensity from well to wake was 7.2 gCO_2 eq/MJ, which is a big drop from the 89 g CO_2 eq/MJ that is usually seen in regular petroleum jet fuel. The minimum fuel selling price was between $1.01 and $1.32 per liter, which means that the process might be close to being able to sell drop-in sustainable aviation fuel (SAF) on the market. The authors also did a sensitivity analysis that showed that the source of hydrogen (especially emissions from steam methane reforming) and the makeup rate of the catalyst might change the GHG results by about ±1.4 g CO_2 eq/MJ and ~2 g CO_2 eq/MJ, respectively. Still, the approach had a low emissions profile even with these changes. In general, this DMCO-based process is very good for the environment and the economy. This is mostly because it uses process intensification to combine direct isoprene fermentation with fewer unit operations, which makes it more efficient and sustainable than other biomass-based or fossil-derived pathways [25].

Budsberg et al. created a one-of-a-kind bioconversion-based jet fuel pathway using poplar biomass. This process includes dilute acid pretreatment, enzymatic hydrolysis, and fermentation by acetogenic bacteria to make acetic acid, which is then distilled, hydroprocessed, and oligomerized into drop-in hydrocarbon jet fuel. They came up with two ways to meet the need for hydrogen: natural gas steam reforming and lignin gasification. Either natural gas or hog fuel might provide the extra heat. Their well-to-wake assessment showed that the global warming potential is between 60 and 66 g CO_2-eq/MJ when utilizing natural gas steam reforming and between 32 and 73 g CO_2-eq/MJ when employing lignin gasification. Fossil fuel use (FFU) goes from 0.78 to 0.84 MJ/MJ in the case of natural gas and from 0.71 to 1.0 MJ/MJ in the case of lignin gasification. The study underscores that hydrogen production is the primary catalyst for both greenhouse gas emissions and fossil fuel consumption, demonstrating that substituting natural gas with hog fuel for heating can substantially mitigate both impact categories. Additionally, bio-jet fuels made from poplar consistently did better than petroleum jet fuel in lowering both GWP and FFU, especially when lignin gasification and hog fuel were used in integrated biorefinery systems [26].

Table 1 summarizes the works that have been done on jet fuel production from biomass resources, along with their key findings.

Table 1. Overview of Biomass-Based Jet Fuel LCA Studies.

Reference	Feedstock	Conversion Pathway	GWP (g CO_2-eq/MJ)	Economic Insights	Sensitivity Parameters
Liu & Yang (2023)	Agricultural residues (corn stover, wheat straw, etc.)	Gasification/Fast Pyrolysis + FT or ATJ	17.9	N/A	H_2 & methanol source, land use, transport
Pierobon et al. (2018)	Slash-pile woody biomass	Fermentation or Gasification + FT or ATJ	26	N/A	Slash pile burning, allocation method
Ahire et al. (2024)	Forest residues	Gasification + FT	24.6	\$1.44/L	Soil carbon change, logistics
Moretti et al. (2022)	Potato by-products	Various upgrading strategies (Attributional & Consequential LCA)	~60% reduction (attributional)	Varies by feed substitution	Feed substitution, allocation assumptions
Han et al. (2013)	Corn stover, oilseeds	HRJ, FTJ, and pyrolysis	Up to 89% reduction (FTJ)	N/A	Feedstock, H2 source, carbon capture
Batten et al. (2024)	Corn stover	Isoprene fermentation + dimerization + hydrotreatment	7.2	\$1.01–1.32/L	H_2 source, catalyst rate
Budsberg et al. (2016)	Poplar biomass	Pretreatment + hydrolysis + fermentation + hydro processing	32–73	N/A	Hydrogen source, heat source

2.4. Gap in Research: Jet Fuel from MSW via FT Synthesis

While several works have been conducted on the development and analysis of various MSW-to-chemical/fuel technologies, limited research is focused on the utilization of this waste feedstock for jet fuel production. Most studies emphasize biogas, ethanol, or electricity. Hence, in this work, an integrated model is developed for the process simulation, cost analysis, and lifecycle environmental impacts assessment of MSW conversion to jet fuel. One of the key challenges of the MSW conversion processes is their low carbon conversion to product and high GHG emissions. Therefore, in this project, the conversion plant is integrated with a CO_2 capture and conversion unit based on the reverse-water-gas shift reaction. Furthermore, to maximize the jet fuel production and reduce other byproducts, an integrated FT-multistage hydrocracking system is designed to attain a product portfolio that is dominated by jet fuel and diesel. Hence, the proposed system can be used to decarbonize the two challenging sectors, the aviation industry and heavy road transport.

Chapter 3- Process Description

This study presents a pathway for converting municipal solid waste into jet fuel through a series of processes. The system is divided into four major units: (1) Drying and Gasification, (2) Treatment, (3) RWGS, and (4) FT synthesis, as represented in the block flow diagram in Figure 2. The process simulation is conducted using Aspen Plus V14. We design an MSW drying system, and the dried MSW can then be used as the feed of the gasification unit to produce high-quality syngas with minimum GHG emissions. To clean the impurities and convert the excess CO_2 into CO, the syngas is then passed through treatment and reverse water-gas shift units, respectively. In order to turn our syngas into jet fuel, FT synthesis is used, during which carbon-based materials are converted into an oil product.

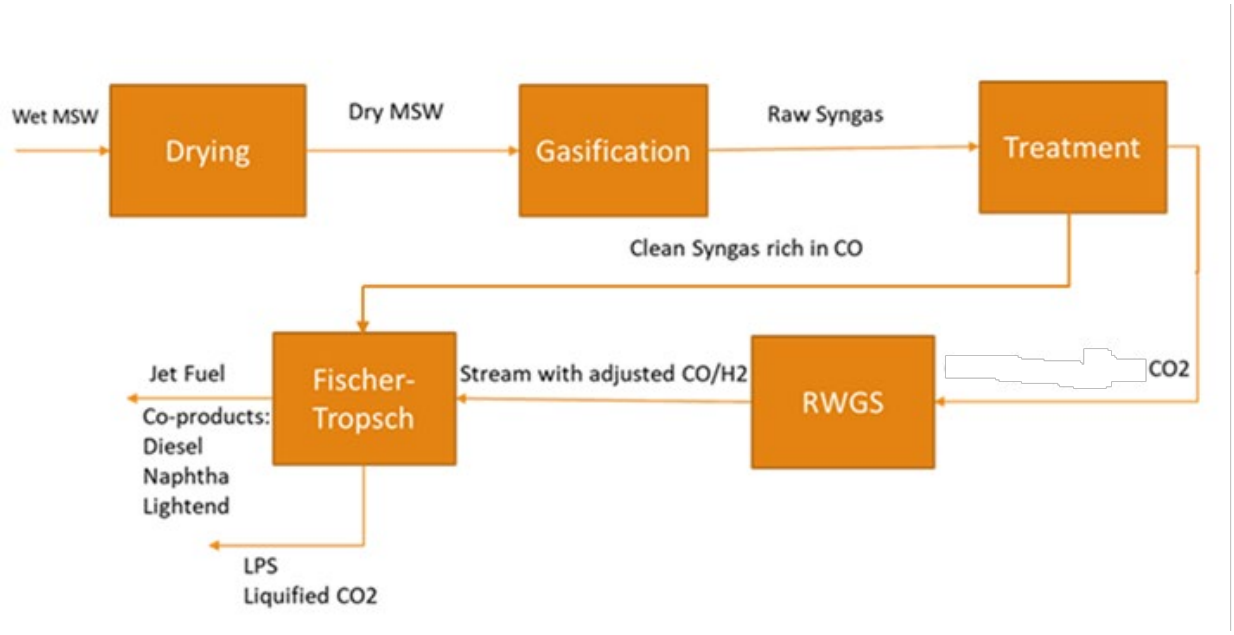

Figure 2- BFD of the process

The operating conditions of each process unit are detailed in their related section; however, a summary of the design specifications and assumptions is listed in Table 2.

Table 2. Main process design parameters of each unit

Unit	Value/Assumption
Gasification	
Gasification reactor	Shell Gasifier modeled as Gibbs (equilibrium) reactor [27]; T=1100℃; Carbon conversion>99.9%
Treatment	
COS hydrolysis	T=193℃; COS removal=100%
Amine system	H_2S removal =99.97%; CO_2 removal=99.98%
Absorber column	21 equilibrium stages; murphree efficiency=33%
Stripper column	30 equilibrium stages; partial vapor condenser; kettle reboiler; murphree efficiency=50%; design spec of DGA mass recovery=96%
RWGS	
RWGS reactor	T=550℃; number of tubes=200; tube length=1m; tube diameter=0.04m; bed voidage=0.55; catalyst density= 5.904gm/cc
FT	
FT reactor	Stochiometric reactor; ASF distribution; $\alpha = 0.95$; CO conversion= 63%; T=220℃; P=20bar

Hydrocracking	
Hydrocracking reactor	Multistage adiabatic RPlug reactor; T=350℃, number of tubes=500; tube length=0.01m; tube diameter=0.0254m; bed voidage=0.5; density of catalyst=1.987 gm/cc; reactor volume= 2.53 m^3
Distillation	Based on ASTM D86: Boiling point for jet fuel cut=180-250℃; boiling point for naphtha cut=100-180℃; boiling point for diesel=250-360℃

3.1. Municipal solid waste feedstock

Figure 3 from the Government of Canada was used to estimate the mass flow rate of MSW. It says that in 2018, the average amount of residential trash thrown out per person was about 694 kg per year [28]. Utilizing Figure 3 and the fact that Montreal has over 1,780,000 people living there, the total amount of MSW produced by homes each year is about 1.235 million tonnes. If it runs all year, this is about 141,000 kg/h, which is what the Aspen Plus simulation uses as the basis for the input feed stream. This flow rate shows that MSW could be a good source of sustainable feedstock for large-scale waste-to-fuel projects in cities.

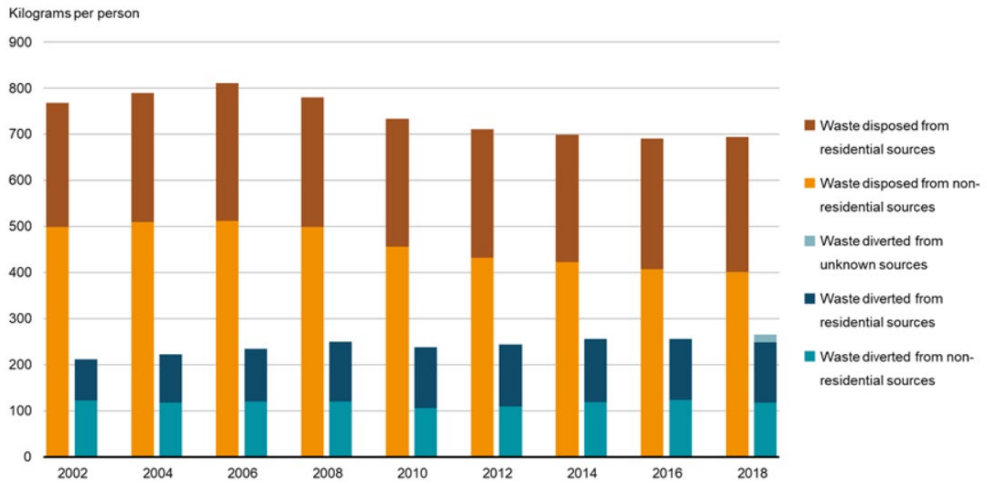

Figure 3. Solid waste diversion and disposal per person, Canada, 2002 to 2018 [28]

The composition of the input MSW, including its ultimate and proximate analyses, is presented in Table 3.

Table 3- MSW data and composition

Parameter	Value
Mass flow rate (kg/hr)	141,000
Heating value (MJ/kg) [29]	16.9
Ultimate analysis (wt%)	Ash: 33.7 Carbon: 36.1 Hydrogen: 5.5 Nitrogen: 1.0 Sulfur: 0.4 Oxygen: 23.1
Proximate analysis (wt%)	Moisture: 50.2 FC (fixed carbon): 33.3 Volatile matter (VM): 3 Ash: 33.7

The higher heating value (HHV) of the feedstock was estimated using a commonly applied empirical correlation based on elemental composition seen in Equation 8. The equation relates the HHV to the mass fractions of carbon (C), hydrogen (H), oxygen (O), nitrogen (N), and sulfur (S) in the material. This formula provides a reliable estimate of energy content for solid fuels such as MSW based on ultimate analysis.

$$HHV = 0.3516C + 1.16225H - 0.1109O + 0.0628N + 0.10465S \ [29] \quad (8)$$

3.2. Gasification Unit

Gasification is the first important step in the process of turning municipal solid waste into jet fuel. It turns the feed into synthesis gas (syngas). The first step in this technique is to dry the input. Wet MSW has a lot of moisture in it, which makes it less efficient at converting heat. To get rid of this extra moisture, wet MSW is pre-treated. A separate drying unit is used in Aspen Plus to dry the material. This cuts the moisture content by around 50% which is the same moisture content as coal, based on the NETL report [27].

After the drying stage, carbon dioxide is added to the pre-treated MSW to make it easier to pressurize the feed stream. The combination is then put through a yield reactor, which is the first step in breaking down complex solid waste into simpler parts, such as water vapor (H_2O), ash, elemental carbon (C), and oxygen (O_2). This breakdown makes it easier to create a more accurate simulation of gasification reactions in Aspen Plus.

After the MSW has broken down, it is mixed with oxygen and high-pressure steam (HPS) and put into a Gibbs reactor. This reactor simulates the gasification process under equilibrium conditions

by minimizing Gibbs free energy. The gasifier works at a temperature of 1100°C, which was chosen based on what the literature says are the best circumstances for getting the most carbon to turn into syngas. The gasifier turns the feed into a raw syngas mixture that is mostly made up of carbon monoxide (CO), hydrogen (H_2), carbon dioxide (CO_2), and methane (CH_4).

The bottom of the gasifier separates solid byproducts, mostly slag or ash. Some of the raw syngas that is made is compressed and sent back to the gasifier to help keep the reaction stable and the temperature steady. The rest of the syngas goes to the downstream treatment unit to be cleaned.

The gasification unit is also thermally connected to the plant's utility system by high-pressure steam (HPS) and boiler feedwater (BFW) loops. The gasifier recovers extra thermal energy, which is then used to make HPS. This is then sent to other high-temperature units in the process. The condensate is recycled as BFW, which improves thermal efficiency and cuts down on the need for outside energy sources.

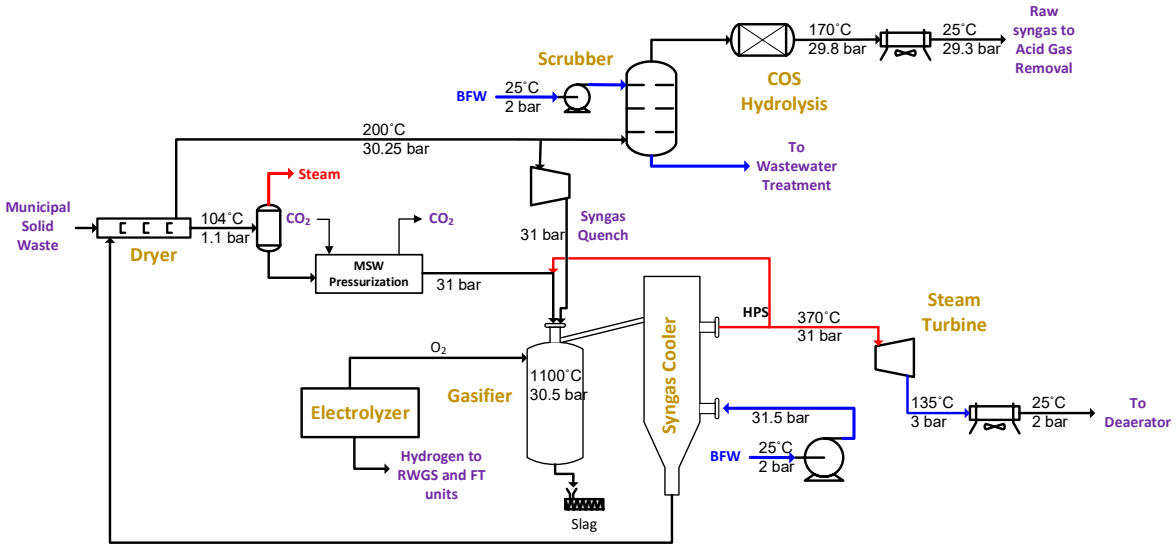

Figure 4. Gasification unit

Table 4 represents some of the parameters that have been achieved after the gasification unit. This shows that from the 141,000 kg/h wet MSW, approximately 98,475 kg/h raw syngas is produced, which will be further processed in the next units.

Table 4. Some parameters of the raw syngas stream

Raw syngas parameters	Values
Flowrate (kg/hr)	98,475.5
Temperature (°C)	200
Pressure (bar)	30.2
CO/H_2	0.9
Component mole fractions	CO: 0.290
	H_2: 0.308
	CH_4: 0.0006
	CO_2: 0.118

3.3. Gas Treatment Unit

Following gasification, the raw syngas, composed primarily of carbon monoxide (CO), hydrogen (H_2), carbon dioxide (CO_2), methane (CH_4), and minor impurities such as hydrogen sulfide (H_2S), carbonyl sulfide (COS), and moisture, is directed to the syngas treatment unit. The primary objectives of this section are to remove acid gases and other contaminants to ensure that the syngas meets the purity specifications required for downstream processes, particularly FT synthesis and the RWGS reactor.

3.3.1 Scrubbing Section

The first step in the treatment process is a physical scrubbing stage, where the syngas is washed with water to get rid of water-soluble and condensable contaminants such as ammonia, trace metals, and particle matter. Before entering the scrubber, water is first pressured to match the pressure of the syngas system. This makes sure that the scrubber works well and removes impurities. The cleaned syngas leaves the top of the scrubber and goes to downstream processing units, while a wastewater stream with the separated pollutants is taken from the bottom for further treatment. A separator and a water wash system work together to get the syngas ready for the next steps in the conversion process by making sure it is clean and at the right temperature.

3.3.2. COS Hydrolysis

After the scrubbing phase, the treatment process proceeds with the hydrolysis of carbonyl sulfide (COS) into hydrogen sulfide (H_2S) and carbon dioxide (CO_2). This makes it easier to separate the sulfur since it changes COS into a form that is easier to separate. At this point, the syngas is sent to a fixed-bed reactor where it is mixed with steam to break down the COS. A stoichiometric reactor with fractional conversion is used, representing the following reaction in Equation 9:

$$COS + H_2O \rightarrow H_2S + CO_2 \quad (9)$$

After the reactor, the syngas stream goes via a heat exchanger to cool the gas to the right temperature for processing downstream. This makes sure that sulfur is handled properly while getting the syngas ready for the next steps in the system.

3.3.3. Acid Gas Removal (Amine System – DGA)

The syngas goes through a two-step chemical absorption and regeneration process using diethanolamine (DGA) as the solvent. This is done to lower the levels of acid gases, especially hydrogen sulfide (H_2S) and carbon dioxide (CO_2). DGA is a tertiary amine that is often used to remove acid gases because it dissolves easily in water, is stable at high temperatures and in chemical reactions, and can be employed again in cycle operations. It only reacts with acid gases through reversible chemical reactions, making weakly bound molecules that can be broken down by heat during regeneration.

The process starts in a RADFRAC absorber column with 21 equilibrium stages. In this column, raw syngas flows up while an aqueous DGA solution flows down, making contact with the syngas. When the pressure and temperature are just right, acid-base interactions and chemical complexation cause H_2S and CO_2 to be absorbed into the DGA solvent. The cleansed syngas, which no longer has acid gas impurities, leaves the top of the absorber and is then compressed and heated up for use in catalytic units downstream. The treated syngas meets downstream purity standards, especially for Fischer–Tropsch synthesis, by having H_2S levels below 5 ppm.

The amine solution that comes out of the bottom of the absorber is transferred to a RADFRAC stripper (desorber) column with 30 equilibrium stages. The solvent is heated here, usually with reboiled steam, which makes the acid gas species come out of the solution. H_2S and CO_2 make up most of the overhead stream. These gases are separated so they may be handled or stored. The regenerated DGA solvent is cooled and sent back to the absorber column in a closed-loop system that keeps everything running smoothly, makes the solvent work better, and saves money. A group of reversible chemical equilibria controls the absorption and regeneration reactions. In the absorber, reactions occur to create bicarbonate and protonated DGA species. In the stripper, these species break down to liberate free CO_2 and H_2S. The main chemical equilibria and their respective thermodynamic constants (A, B, and C) are summarized in Table 3. These constants follow the Van't Hoff-type correlation as shown below:

$$\ln(Keq) = A + \frac{B}{T} + C \times \ln(T) \quad (10)$$

where Keq is the equilibrium constant and T is the absolute temperature in Kelvin. The reactions include:

- Protonation of DGA and H_2O to form DGA^+ and H_3O^+
- Formation of bicarbonate from dissolved CO_2
- Reversible formation of hydrosulfide (HS^-) and its protonation
- Additional minor reactions with hydroxide ions and carbonate species

These reactions from Table 5, taken from the Aspen Plus database, reflect typical behavior in acid gas absorption systems.

Table 5. Equilibrium Reactions and Constants for DGA-Based Acid Gas Absorption in the Absorber Column

Reaction	Equilibrium constant A	Equilibrium constant B	Equilibrium constant C
$H_2O + DGACOO^- \leftrightarrow DGA + HCO_3^-$	3.66	-3,696.16	0
$H_2O + DGA^+ \leftrightarrow DGA + H_3O^+$	-13.33	-4,218.70	0
$H_2O + HCO^{3-} \leftrightarrow CO_3^{--} + H_3O^+$	216.05	-12,431.70	-35.48
$2H_2O + CO_2 \leftrightarrow HCO_3^- + H_3O^+$	231.46	-12,092.09	-36.78
$H_2O + HS^- \leftrightarrow H_3O^+ + S^-$	-9.74	-8,585.46	0
$H_2O + H_2S \leftrightarrow H_3O^+ + HS^-$	214.58	-12,995.40	-33.54
$2H_2O \leftrightarrow OH^- + H_3O^+$	132.89	-13,445.90	-22.47

After the amine treatment, the clean syngas is compressed and heated up for use further down the line. This system is made to get the H_2S levels in the treated syngas below 5 ppm, which is what the high purity standards for the next catalytic processes call for. After treatment, the syngas is separated into two product streams based on what the process needs:

1. CO_2-Rich Stream → RWGS Unit: Some of the cleaned syngas, which has more CO_2 in it, is sent to the RWGS reactor. Here, the H_2/CO ratio of the syngas is modified again to get it ready for FT synthesis. CO_2 is used as part of the feed.

2. CO-Rich Stream → FT Unit: The rest of the syngas, which has less CO_2 and more CO and H_2, goes to the FT synthesis unit, where it is turned directly into liquid fuels with little need for further conditioning.

This amine-based treatment system makes sure that acid gases are always removed, which lets the RWGS and FT units use the syngas more efficiently while keeping operational costs low.

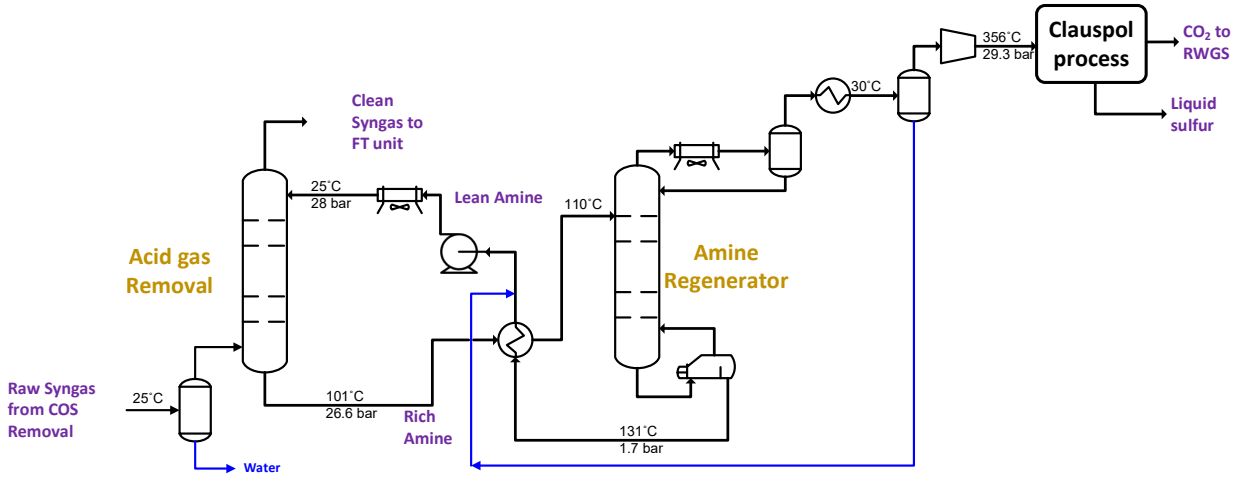

Figure 5. Acid gas removal unit

The effectiveness of the acid gas removal system is reflected in the significant reduction of key impurities following treatment. As shown in Table 6, the concentration of hydrogen sulfide (H_2S) in the syngas was reduced from approximately 3,244 ppm (mass fraction ~3.24×10^{-3}) to just 4.39 ppm (mass fraction ~4.39×10^{-6}), achieving more than 99.9% removal efficiency. Carbonyl sulfide (COS) and elemental sulfur were entirely eliminated, while ammonia (NH_3) levels were reduced by several orders of magnitude. These results confirm the system's ability to meet strict purity specifications, particularly for sulfur-sensitive downstream units like the FT reactor. Table 7 shows the most important features of the processed syngas stream. The syngas leaves the acid gas removal section at a temperature of around 14°C and a flow rate of about 45,885 kg/h. The H_2/CO ratio is changed to about 1.06, which made it perfect for either RWGS or FT synthesis, depending on how the streams were split.

Table 6. Mass fraction of impurities before and after treatment

Component	Raw Syngas (mass fraction)	Clean syngas (mass fraction)
S	2.2E-10	0
H_2S	3.2E-03	4.4E-06
COS	1.0E-04	0
NH_3	7.5E-05	3.4E-13

Table 7. Some parameters of the clean syngas

Parameter	Value
Flowrate	45,884.9
Temperature	13.9
H_2/CO	1.06

3.4. Reverse Water Gas Shift (RWGS) Unit

The RWGS unit is very important for changing the H_2/CO ratio of the syngas so that it is at the right level for Fischer–Tropsch synthesis. In this unit, a stream of CO_2 that has been recycled from the treatment unit is mixed with hydrogen to make more carbon monoxide and water through the Reverse Water-Gas Shift reaction, based on Equation 11:

$$CO_2 + H_2 \rightarrow CO + H_2O \quad (11)$$

This endothermic reaction turns CO_2 into a reactive syngas component (CO), which makes better use of carbon and makes the whole process more efficient. In Aspen Plus, the RWGS reactor is represented with a specialized kinetic reactor that works in the vapor phase. This gives you more control over reaction rates, equilibrium conditions, and how the different parts of the reactor interact with each other.

As shown in Figure 6, the CO_2 input enters the reactor system at about 357°C and 28 bar. Hydrogen, on the other hand, is fed in at a lower pressure and temperature and then compressed through a multistage compressor to meet the conditions at the reactor inlet. Before it goes into the RWGS reactor, which runs at about 550°C and 20.8 bar, the mixed stream is preheated. Because the process is endothermic, this high-temperature environment is needed to push the equilibrium toward the creation of CO and H_2O. The rate expression is given by the equation below:

$$Rate\ expression = [Kinetic\ factor][Driving\ force][Custom\ term] \quad (12)$$

Each component of this rate expression is defined as follows:

- The kinetic factor k is defined using an Arrhenius-type expression.
- The driving force is defined by the product of the mole fractions of reactants
- The custom rate expression in Aspen Plus is implemented using mole fractions of the involved species and an equilibrium-based correction factor

Resulting in the following Equation 12:

$$r = k_0 \,.\exp\left(\frac{-E}{RT}\right) \times \frac{(Y_{CO_2}.Y_{H_2}) - \left(\frac{Y_{CO}.Y_{H_2O}}{K_{eq}}\right)}{CFP} \quad (13)$$

where:

- k_0=218,520 mol/gm
- Activation energy E=17.1069 kcal/mol
- $K_{eq} = \exp\left(4.33 - \frac{4577.8}{T}\right)$
- $CFP = \left(\frac{P}{100000}\right)^{0.5-\left(\frac{P}{25000000}\right)}$
- Reaction rate unit is mol/gm·s
- Reaction occurs in the vapor phase
- Y_i terms represent mole fractions of each species (CO_2, H_2, CO, H_2O)

This formulation makes sure that the thermodynamics are consistent while also letting the RWGS reactor's conversion behavior be easily changed to fit different operating situations. After the RWGS unit makes the CO-rich stream, it is mixed with the bypass syngas stream from the treatment unit. The temperature and pressure of this mixed stream are then adjusted before it goes into the FT synthesis block. The RWGS reactor's flexibility to change the H_2/CO ratio easily helps get the most carbon conversion and make the syngas composition just right for the FT unit.
The performance of the RWGS unit is summarized in Table 8, which shows the mass fraction of major components before and after the reactor. The RWGS conversion works because the CO_2 concentration lowers from 0.9829 to 0.4001, and the CO content rises from 0.0007 to 0.2998. We also see an increase in the concentration of water.
Also, we employ a high-temperature Fe–Cr/Al_2O_3 (iron–chromium on alumina) catalyst for RWGS. This formulation delivers fast CO_2→CO kinetics and high CO selectivity in the 500–600 °C window while suppressing methanation; it is also steam/thermal-stable and cost-effective relative to noble metals. The Al_2O_3 support provides dispersion and mechanical strength for fixed-

bed service, and the choice is consistent with RWGS intensification studies that benefit from robust high-T catalysts [30].

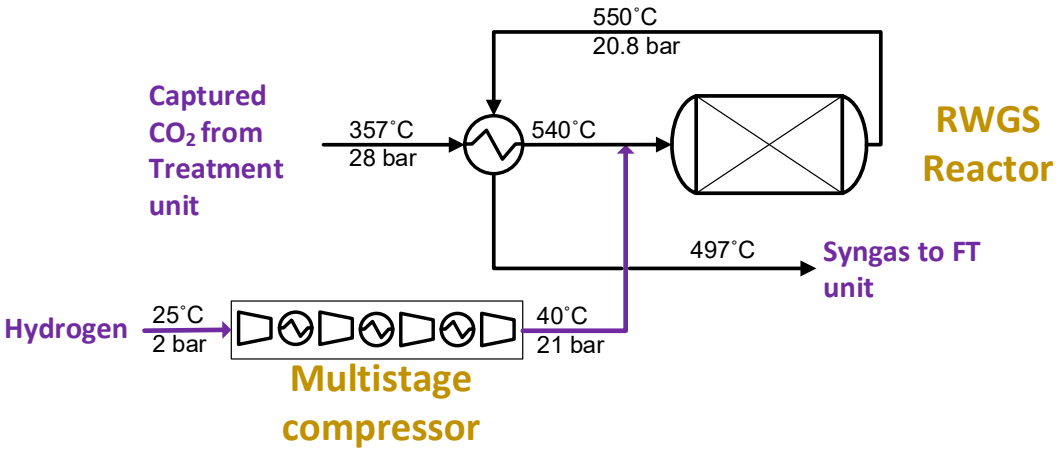

Figure 6. RWGS unit

Table 8. Mass fraction of main components before and after RWGS

Component	Before RWGS	After RWGS
CO_2	0.9829	0.4001
H_2	0.0001	0.0932
CO	0.0007	0.2998
H_2O	0.0160	0.2066

3.5. Fischer–Tropsch (FT) Synthesis Unit

3.5.1. FT reaction

The FT synthesis unit is an important part in turning syngas (CO and H_2) into liquid hydrocarbons, which can include chemicals that are used to make jet fuel. This technique uses a catalyst to turn carbon monoxide and hydrogen into long-chain paraffinic hydrocarbons, following the general reaction in Equation 14:

$$(2n+1)H_2 + nCO \rightarrow C_nH_{2n+2} + nH_2O \quad (14)$$

Although the FT synthesis is very exothermic and complicated, several researchers have tried to explain its kinetics using both mechanistic and empirical methods. Van Der Laan and Beenackers (1999) conducted a thorough analysis of FT reaction kinetics, examining intrinsic rate models for

cobalt and iron catalysts. They said that FT synthesis usually follows Langmuir-Hinshelwood-type kinetics, with the adsorption of CO being the phase that slows it down the most. But selectivity and yield are also greatly affected by high temperature, water inhibition, and the chance of chain development [30].

Ma et al. (2014) conducted a focused examination of the water inhibitory effects on cobalt-based catalysts, underscoring the imperative of efficient water removal to sustain catalyst activity and optimize heavy hydrocarbon outputs. Their results show how important reactor design and heat removal methods are, especially in fixed-bed setups [31].

Chang et al. (2007) simulated FT kinetics in a slurry-phase reactor utilizing a Fe–Cu–K–SiO_2 catalyst. Their kinetic expression encompassed terms for both CO and H_2 adsorption and desorption, while also considering competing water–gas shift (WGS) processes, which are particularly significant when employing iron-based catalysts. However, because FT kinetics are quite complicated and depend on the catalyst, this study, like many others, came to the conclusion that no universal kinetic model can explain all reaction dynamics when conditions change [32].

Due to these complications and the diverse operating regimes, this study chose not to include full kinetic expressions in the Aspen Plus simulation. Instead, a stoichiometric reactor method was used, with overall conversion and selectivity values taken from literature and experimental benchmarks.

The Anderson–Schulz–Flory (ASF) probability distribution was used to predict the chain-growth behavior of FT synthesis products in order to accurately approximate the distribution of hydrocarbons. The ASF model presumes a uniform chain-growth probability, α, applicable to all product sizes, facilitating the determination of molar fractions of C_1–C_n hydrocarbons. The probability function is given as an equation below:

$$W_n = (1-\alpha).\alpha^{n-1} \tag{15}$$

Where W_n is the molar fraction of hydrocarbons with carbon number n, and α is the chain growth probability, typically ranging from 0.85 to 0.95 depending on catalyst and operating conditions.

For this investigation, we chose a chain growth probability of α = 0.95. This value aligns with previous findings regarding cobalt-based low-temperature Fischer-Tropsch catalysts, recognized for promoting the synthesis of heavier hydrocarbons, especially within the C_8–C_{16} range linked to jet fuel. The modeling method used here is similar to the one used by Eilers et al. (1990) to describe the Shell Middle Distillate Synthesis (SMDS) process. For their industrial FT application, a cobalt catalyst is used at low temperatures (around 200–240°C) to get the most middle distillate. The average temperature of 220°C was used. Their stated α-values likewise range from 0.93 to 0.95, which supports the choice of distribution in this work. Based on this distribution, the hydrocarbon spectrum has about 8.6% C_1–C_9, 19.8% C_{10}–C_{20} (middle distillates), and 71.7% C_{20}+ wax fractions by weight [33], aligning with the desired fuel product slate. Table 9 summarizes some of the design parameters used for designing the FT reactor.

As shown in Figure 7, after the reaction, the effluent from the FT reactor is cooled and sent to a three-phase separator, where it is divided into three parts:

- A liquid hydrocarbon phase, rich in FT waxes and heavy products,
- An aqueous phase, primarily containing water formed during the FT reaction,
- A gas phase, consisting of unreacted syngas and light hydrocarbons.

First, the aqueous phase is decanted to reduce the extra water. This water is then either purged or recycled, depending on what the process needs. Some of the light gas phase is sent back to the reactor to help the carbon use and keep the H_2/CO balance, while some of it is sent to an oxyfuel boiler to get rid of the accumulation of light gases.

The FT liquid product, which has a lot of waxes (C20+), goes to the hydrocracking unit to be turned into hydrocarbons that are in the jet fuel range. The system also has a steam generation loop, which uses some of the process heat to make low-pressure steam, which makes the whole system more energy efficient.

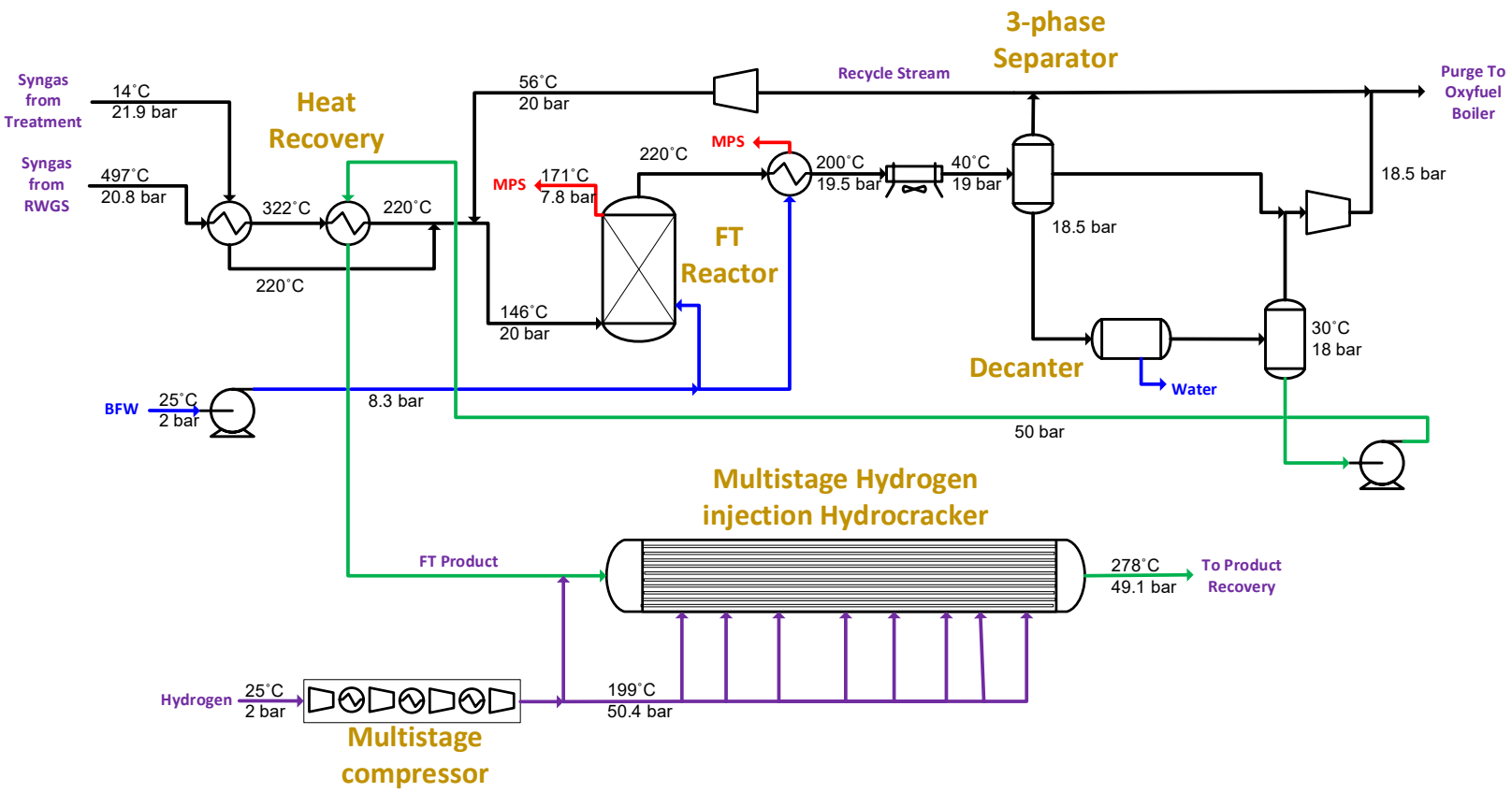

Figure 7. Process flow diagram of FT and Hydrocracking sections of the FT unit.

Table 9. Design parameters of the FT reactor

Properties	Values
Temperature (°C)	220
Pressure (bar)	20
Fractional CO Conversion	0.63
Alpha [33]	0.95

3.5.2. Hydrocracking

To enhance the yield of jet fuel-range hydrocarbons (C_8–C_{16}), the heavy paraffins and waxes produced in the Fischer–Tropsch reactor are routed to a hydrocracking unit. In order to have better temperature control, a multi-stage hydrogen-injection hydrocracking reactor is used for simulation, where each one represents a segment of an industrial hydrocracking reactor. More than 35 stoichiometric hydrogenation and cracking processes were done on paraffinic hydrocarbons with carbon chains from C_2 to C_{64}. These reactions mimic the process of turning heavier hydrocarbons into lighter, more useful fractions like kerosene and diesel-range products.

For instance, reactions like $C_2H_6 + H_2 \rightarrow 2\ CH_4$ and $C_3H_8 + H_2 \rightarrow C_2H_6 + CH_4$ illustrate primary hydrogenolysis, while reactions such as $C_{10}H_{22} + H_2 \rightarrow 2\ C_5H_{12}$ and $C_{28}H_{58} + H_2 \rightarrow 2\ C_{14}H_{30}$ simulate deep cracking of long-chain paraffins.

Before going into the hydrocracking phase, the FT product stream is heated up with high-pressure hydrogen and combined with it. Each part of the reactor works at high pressure (about 50 bar) and rising temperatures, from about 232°C to about 275°C. This makes it easier for heavy hydrocarbons to split into lighter fractions.

Each reaction was embedded in a custom reaction class with independently defined rate expressions. The kinetic model follows a generalized power-law form, where the driving force is represented by the product of reactant concentrations raised to their respective reaction orders, evaluated in the vapor phase using either partial pressure or molarity, depending on the specific reaction. Each reaction rate is modeled using an Arrhenius-type rate expression of the form, resulting in Equation 16:

$$r = A \times exp(1.8765 + 0.6255n) \times exp(40.48 - \frac{25819.68}{T}) \times M_{reactants} \times V_{reactor}^2 \times \rho_{catalyst} \quad (16)$$

Where:

- A=0.001819
- n is the carbon number of the hydrocarbon reactant
- T is the absolute temperature (Kelvin)
- M is based on the summation of molarities of reactants in the liquid and vapor phase (kmol/$m^{3)}$
- V is the volume of the reactor (m^3)
- ρ is the density of the catalyst (kg/m^3)

These rate constants and expressions are adapted from the kinetic model proposed by Teles and Fernandes (2008) [34], specifically designed for the hydrocracking of FT waxes into naphtha and diesel-range products. We use the defined kinetic equations to figure out the reaction rates for each species. We then keep track of these rates throughout all RPlug segments using volume and concentration-dependent parameters.

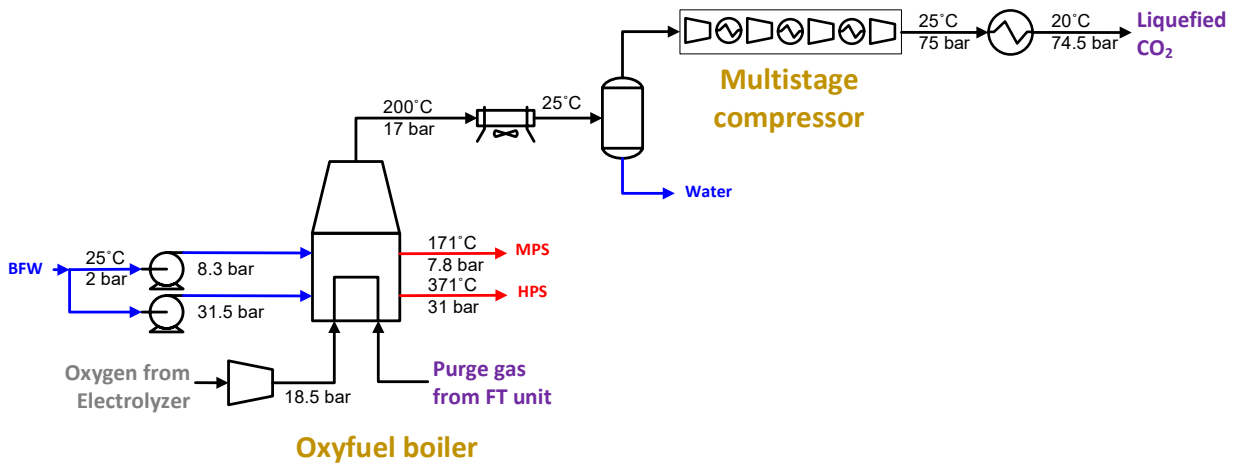

Figure 8. Purge gas oxyfuel combustion and CO_2 liquefaction sections.

Figure 8 shows the parts of the process that deal with integrated purge gas oxyfuel combustion and CO_2 liquefaction. The main goal of this unit is to use the purge gas that comes out of the Fischer–Tropsch unit to get energy back and capture CO_2 so it can be turned into a liquid later. In the combustion stage, the purge gas goes to an oxyfuel boiler, where it is burned with pure oxygen from an electrolyzer. Boiler feed water is also sent to the boiler. It starts at 25°C and 2 bar and is then pumped to 8.3 bar and finally to 31.5 bar. The combustion process creates flue gases that are very hot. These gases are utilized to make two types of steam: medium-pressure steam (MPS) at 171°C and 7.8 bar, and high-pressure steam (HPS) at 371°C and 31 bar. This steam is used in other sections of the process to recover thermal energy and make it work better.

After the steam is made, the flue gas goes through a cooling stage where its temperature is lowered to 25°C. This is the process where water is removed from the system by condensation. After that, a multistage compressor compresses the leftover gas, which is high in CO_2. After that, the high-pressure CO_2 stream is cooled to 20°C in a condenser, which lowers the pressure somewhat to 74.5 bar. In these conditions, CO_2 is turned into a liquid and stored or used. This setup makes it easy to capture carbon and get back useful thermal energy in the form of steam. It is an important aspect of the whole process of turning waste into jet fuel.

3.5.3. Distillation column

After hydrocracking, the feed stream is initially cooled down and heated up by heat exchangers before going into the fractionation column. The improved product stream goes to a distillation unit that uses the PetroFrac column in Aspen Plus to separate the hydrocracked mixture into specific product fractions. The column has 25 theoretical stages and a reboiler at the bottom. It also has a built-in side-stripper to improve separation efficiency and product purity.

The main goal of the distillation section is to get back as much of the C_5^+ hydrocarbon fraction as possible as jet fuel (C_8–C_{16}), in line with the middle-distillate yield for the Shell SMDS process [33], and to meet ASTM D86 atmospheric distillation standards for jet fuel quality.

The product cuts are based on boiling point standards. The jet fuel fraction is usually recovered at around 220°C, while lighter hydrocarbons are recovered as naphtha and gaseous light ends, and heavier fractions are retrieved as diesel.
Also, steam is injected at the bottom of the column to help with stripping and make the differences in volatility bigger, which makes it easier to separate components and lowers the duty of the reboiler. To get the most jet fuel back, bottoms and reboiler tasks are set up so that heavier parts don't get into the cut. According to ASTM D86 [35] boiling point cut ranges:

- Naphtha: ~100–180°C,
- Jet fuel (kerosene cut): ~180–250°C,
- Diesel: ~250-360°C.

This fractionation strategy makes it possible to make jet fuel that meets fuel certification standards while getting the most out of the lighter and heavier fractions and keeping operational efficiency high. This makes sure that the fuel products downstream meet their target specifications for further refining or direct use.

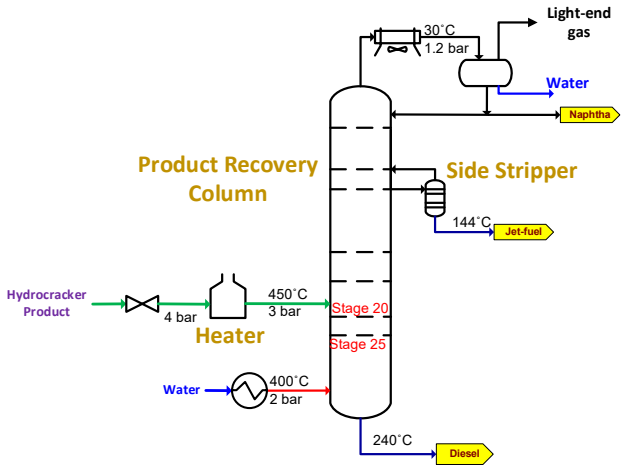

Figure 9. Fractionation section of the FT unit.

The last step of the process separates about 22,000 kg/h of processed hydrocracker product into different fuel fractions and by-products in the product recovery column (Figure 9). Kerosene (10,489 kg/h), diesel (9,603 kg/h), naphtha (449 kg/h), and light ends (667 kg/h) are the main hydrocarbon outputs. Water (26.7 kg/h) is also recovered as a minor by-product. This distribution shows that kerosene and diesel make up more than 90% of the total hydrocarbon output. This shows that the process is focused on making intermediate distillates. Lighter components like naphtha are taken from the top, jet fuel (kerosene range) is taken from the side, and diesel is taken from the bottom.

Chapter 4- Results

In this chapter, first, the simulation results are presented and discussed. Then, using the simulation results, a comparative lifecycle assessment of the process is conducted and the LCA results are compared with other jet fuel production pathways. Finally, the detailed techno-economic analysis of the plant is conducted to evaluate the financial viability of the process at different market conditions.

4.1. Process simulation results

A summary of the simulation results of the proposed waste-to-jet fuel conversion pathway is presented in this section. The system is designed to treat 141,000 kg/h of wet MSW, which undergoes a series of integrated thermal, catalytic, and separation units. The simulation has important steps, including drying the MSW, gasifying it to make raw syngas, cleaning and adjusting the syngas, using Fischer–Tropsch synthesis to make long-chain hydrocarbons, and finally hydrocracking and fractional distillation to separate the products. The data in Table 10 demonstrate that the process makes a variety of useful products, such as 50% kerosene-range hydrocarbons (the desired jet fuel product), 45% diesel, 2% naphtha, and 3% light ends. Along with fuels, a lot of liquefied CO_2 is also collected (28,327.2 kg/h). This CO_2 can be stored or used, depending on how it will be used later. The process also makes 96,235.1 kg/h of low-pressure steam, which might be sold to be used for heating. These simulation results are the basis for the next techno-economic and life cycle studies, which will let us fully evaluate the proposed MSW-to-jet fuel pathway.

Table 10. Summary of simulation results

Data		Mass flow (kg/hr)	LHV (MJ/hr)
Input			
	MSW	141,000	1,182,290
Outputs			
	Kerosene	10,489.3	464,475.5
	Diesel	9,602.8	422,462.9
	Naphtha	449.1	19,908.3
	Lightened	666.7	17,835.8
	Liquified CO_2	28,327.2	0
	LPS	96,235.1	0
Total electricity demand (MJ/hr)		1,062,625.7	

Table 11 shows the simulation results for electricity use across the main process units. It shows that gasification is the only unit that makes more electricity than it uses, making about 3,421.7 MJ/h, mostly by recovering heat and making steam as part of the system. On the other hand, all

the other units use more electricity than they produce. The RWGS reactor uses the most energy, followed by Fischer–Tropsch synthesis and syngas treatment. Electrolysis uses more than 99% of the system's total electricity, which shows how much energy is needed to make hydrogen from water splitting. These numbers show how important electrolysis is to the overall energy balance and how important it is to include electricity generation from gasification to help meet some of the process's electrical needs.

Table 11. Electricity consumption of each process unit

Electricity consumption (MJ/hr)	**Results**
Gasification and steam turbine	-3,421.7
Treatment	2,046.1
RWGS	6,438.6
FT	2,044.5
Electrolysis	1,055,518

We evaluated the total lower heating value (LHV) of the product outputs to the total energy inputs to see how energy-efficient the system was. The energy inputs were the LHV of the wet MSW feedstock and the electrical needs of critical units such as gasification, treatment, RWGS, Fischer–Tropsch, and hydrogen generation. The LHV of the system's primary products, which are kerosene, diesel, naphtha, and light ends, is what the energy outputs are. The simulation results suggest that the process has a net energy efficiency of 41% (LHV basis), as shown in Table 12. This means that 41% of the energy used in the operation is transformed into usable fuel products. This shows that the integrated system can extract a good amount of energy from municipal solid waste while creating low-carbon fuels. This supports its use as a way to turn waste into something useful that doesn't require a lot of energy.

Table 12. Summary of energy efficiency

Inputs, MJ/hr		**Value**
	Wet MSW	1,182,290
	Total electricity demand	1,062,625.7
Total		**2,244,915**
Outputs, MJ/hr		
	Kerosene	464,475
	Naphtha	19,908
	Diesel	422,463
	Light end	17,836
	Water	0
	Liquified CO2	0
	LPS	0
Total		**924,683**
Net Efficiency (%LHV)		**41**

4.2. Life cycle assessment

LCA is conducted based on the ISO 14040 standard, which describes the four phases of LCA: goal and scope definition, life cycle inventory analysis, life cycle impact assessment, and life cycle interpretation. Figure 10 shows the system boundary and the main process units that are included in our LCA.

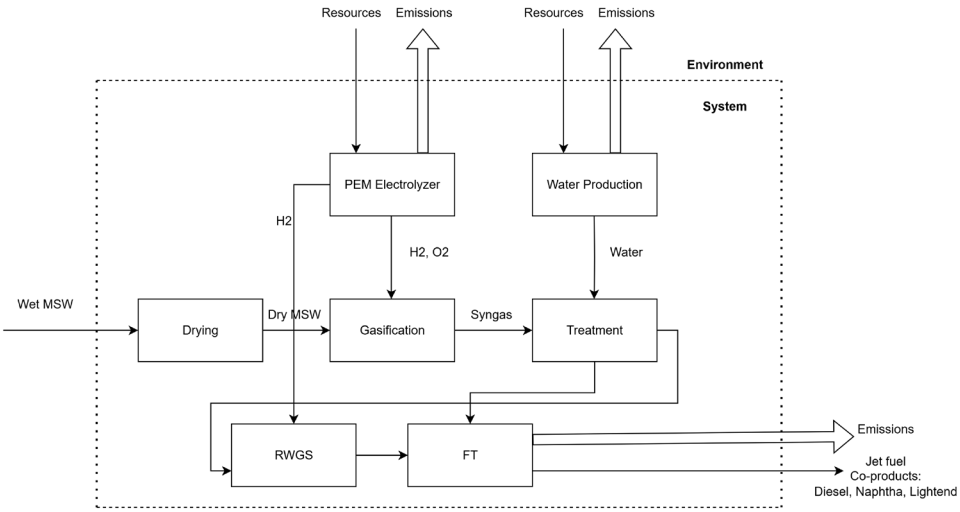

Figure 10. System boundary for LCA study

4.1.1. Goal and scope definition

The main goal of this study is to look at how well a thermochemical approach for making sustainable jet fuel from municipal solid waste works for the environment. The life cycle assessment looks at the effects from a well-to-tank point of view and contrasts the suggested pathway in three different situations:

1. **Conventional fossil-based jet fuel production** – The environmental effects of creating 1 kg of jet fuel through the MSW-based pathway are contrasted with those of traditional fossil-derived jet fuel, simulated in the OpenLCA utilizing the kerosene dataset from the Ecoinvent 3.8 database. This conventional jet fuel inventory is based on a "Rest of World" (R.O.W.) refinery dataset, representing crude oil with an average API gravity of 35 and 1.03% sulfur content, and including all major refinery processes from crude input to refined product output, and serves as a benchmark for comparison. An additional case is evaluated using an energy allocation approach, where avoided product credits are not applied, and environmental burdens are distributed proportionally to the energy content of the main product and co-products.
2. **MSW incineration with energy recovery** – This section compares the environmental effects of turning 1 kg of MSW into jet fuel with those of burning 1 kg of MSW to make

electricity. This scenario examines the advantages of converting MSW into liquid fuels rather than restricting its use solely to energy recovery.

3. **Comparison with alternative bio jet fuel pathways** – The MSW-to-jet fuel results are compared to three bio jet fuel pathways from the literature to see how well they do in different impact categories.

The system boundaries (Figure 10) include: MSW collection and transport, drying, gasification, syngas cleaning, RWGS, Fischer–Tropsch synthesis, hydrocracking, and product separation. Electricity demand for all process steps is included, sourced entirely from the Quebec provincial grid mix. Since the grid is dominated by low-carbon hydroelectric power from Hydro-Québec, its contribution to greenhouse gas emissions is substantially lower than in regions with fossil-intensive generation such as Alberta. Emission factors for the Quebec grid were obtained from the Ecoinvent 3.8 regionalized datasets, which also account for upstream impacts from dam construction, land-use change, and infrastructure maintenance.

Infrastructure construction, plant maintenance, product distribution, and end-of-life stages are excluded, in line with the study's focus on production-phase impacts. Emissions from catalyst manufacturing and minor chemical additives (e.g., solvents, sorbents) are excluded due to their negligible contribution to the total inventory. No environmental credit is assigned for the MSW feedstock; it is treated as a zero-burden input at the system boundary, meaning the advantages observed in the results are attributable to the process performance and co-product displacement rather than to "waste diversion" credits.

The functional unit varies according to the comparison scenario:

- **Scenario 1** – 1 kg of jet fuel produced (mass-based) to match the OpenLCA fossil baseline dataset.
- **Scenario 2** – 1 kg of MSW processed, enabling direct comparison of fuel production and electricity generation from the same feedstock.
- **Scenario 3** – 1 MJ of jet fuel produced, for direct comparison with literature biojet fuel pathways

This scenario-specific functional unit approach ensures methodological consistency while allowing targeted evaluation against relevant benchmarks for each pathway

4.1.2. Life cycle inventory analysis

The inputs and outputs for the life cycle inventory (LCI) came from the extensive process simulations that were discussed in the preceding sections. The simulation included all of the main unit processes, such as drying MSW, gasifying it, treating syngas, the RWGS reaction, FT synthesis, hydrocracking, and separating the end product by distillation.

The modeled process handles about 141,000 kg/h of MSW. This number was figured up using statistics from the Government of Canada on how much waste cities produce and how many people live in Montreal. The simulation gave us information about the efficiency of converting feedstock, the composition of syngas, the use of CO_2, the needs for electricity and steam, and the distribution of products like jet fuel, diesel, naphtha, light ends, and solid wastes. These flow rates and energy balances form the basis of the life cycle inventory and are summarized in Table 13.

The environmental impact of power generation is very important to the overall LCA because several unit operations need a lot of electricity, especially the RWGS, FT synthesis, and compression systems. This study exclusively examines power sourced from Quebec's hydroelectric grid, reflecting the geographical setting of the process. Quebec's electricity comes mostly from hydropower, which has very low greenhouse gas emissions. We got the emission factors for hydroelectricity from OpenLCA 2.4.1 and checked them against provincial LCA reports and peer-reviewed literature.

The inventory also includes material inputs such as oxygen, steam, and water, as well as output emissions, including process wastewaters. By-products such as diesel and naphtha are accounted for as co-products within the system. For the life cycle inventory modeling, an assumption was made regarding the treatment unit’s solvent input (ethanol, 2-(2-aminoethoxy)-), which corresponds to the DGA (diglycolamine) used for CO_2 capture in the syngas treatment unit. Additionally, the “light ends” fraction produced in the process, which is not explicitly defined within the LCA database, was assumed to have the same properties as natural gas for inventory purposes due to similar density and compositional characteristics. Plant construction, infrastructure, and catalyst manufacturing are excluded from the inventory in accordance with the system boundaries defined in Figure 10.

Table 13. LCI inputs and outputs

LCI Inputs (per 1 MJ of jet fuel):		
Flow	**Amount**	**Unit**
Electricity, high voltage, Quebec	101.31	MJ
Oxygen	0.87	kg
Water	0.41	kg
Municipal solid waste	13.44	kg
DGA	1.9E-04	kg
LCI Outputs (per 1 MJ of jet fuel):		
Flow	**Amount**	**Unit**
Jet fuel (product)	1.00	MJ
CO_2, liquid	2.70	kg
Compressed natural gas	0.079	kg
Naphtha, regional storage	6.34E-02	m^3
Diesel, at the refinery	1.1E-03	m^3
Process wastewater	2.5E-04	kg
Steam (co-product/by-product)	9.17	kg

4.1.3. Life cycle impact assessment (LCIA)

We used OpenLCA with the ReCiPe 2016 (Hierarchy) technique to do the life cycle impact assessment for this study. This method was chosen since it covers a wide range of environmental effect categories and works with both midpoint and endpoint interpretations. The midpoint evaluation includes a broad range of indicators such as climate change, fossil resource scarcity, terrestrial acidification, freshwater eutrophication, human toxicity, and ozone formation, that capture specific cause-and-effect mechanisms within the life cycle. These categories provide a detailed understanding of potential environmental pressures at an intermediate stage before they are aggregated into damage-oriented endpoints.

The endpoint evaluation combines the midpoint data into three main damage categories: human health, ecosystem quality, and resource availability. This higher-level interpretation makes it easier for decision-makers to understand the environmental trade-offs because it uses more concrete measures, like disability-adjusted life years (DALYs) for human health or species loss for ecosystems. Also, the resource availability endpoint is shown in dollars (USD 2013), which shows

how resource depletion, especially the lack of fossil fuels and minerals, would affect the economy in the long term.

4.1.4. LCA results

There are two levels of Life Cycle Assessment results for this study: midpoint and endpoint. The midpoint results show how the planned MSW-to-jet fuel process compares to other options in terms of specific environmental effect categories, like global warming, acidification, and ecotoxicity. The endpoint results then group these middle effects into larger damage categories, such as human health, ecosystem quality, and resource depletion. This gives a broader view of how well the process works for the environment as a whole. These data, when taken together, give a full picture of the possible environmental benefits of the suggested pathway from many different points of view and impact categories.

4.1.4.1. Midpoint Results

The midpoint life cycle assessment results are shown for three different comparison scenarios, each of which is meant to show a different part of the planned municipal solid waste MSW-to-jet fuel pathway's environmental performance. We use midpoint impact categories from the ReCiPe 2016 technique to rate all scenarios. This makes it possible to compare different functional units and system boundaries on the same foundation.

Scenario 1 – MSW-to-jet fuel vs. case 1, with conventional fossil jet fuel, and case 2, MSW-to-jet fuel with energy allocation

In the first scenario, the environmental impacts of producing 1 kg of jet fuel via the MSW-based process are compared directly against those of conventional petroleum-derived jet fuel using datasets available in OpenLCA. To account for methodological variations in burden allocation, a third case is also included in which the MSW pathway’s impacts are calculated using energy allocation without avoided product credits. This scenario examines the impact of co-product displacement on net environmental outcomes, elucidating the extent of benefits derived from avoided diesel, naphtha, light hydrocarbon, and CO_2 consumption credits. In the MSW model, the feedstock is regarded as waste, with no environmental costs associated with its production. This guarantees that the differences in results are mainly due to the extraction and processing of fossil resources in the conventional case compared to the utilization of low-burden waste feedstock in the MSW case.

Scenario 2 – MSW-to-jet fuel vs. MSW incineration for electricity generation

In the second scenario, the functional basis changes from the amount of jet fuel to the amount of MSW processed. This makes it possible to directly compare two different ways to turn the same waste feedstock into value: (1) conversion to jet fuel through the proposed process and (2)

electricity generation through conventional incineration. This scenario compares the two approaches based on how much environmental harm they avert, using MJ of product output per 1 kg of MSW as the functional reference. The comparison shows the pros and cons of making a high-value, low-carbon transportation fuel from the same waste stream and making power from it. It focuses on things like how much fine particulate matter is made, how much it could cause global warming, and how much it could cause acidification on land.

Scenario 3 – MSW-to-jet fuel vs. literature-based bio jet fuel pathways

In the third scenario, we compare the midpoint results for the MSW-to-jet fuel pathway to three biojet fuel production routes: palm oil, soybean oil, and waste cooking oil (WCO). For this comparison, all the figures are based on the production of 1 MJ of jet fuel. The bio jet fuel datasets originate from D'Ascenzo et al. (2022), which establishes a uniform methodological framework for cross-feedstock assessment. This comparison shows the differences between a waste-based, non-agricultural approach and crop-based feedstocks, which have greater upstream costs for growing, harvesting, and processing. To make it easier to compare findings from different categories that use different reference units, they are shown as percentages of the highest absolute value found in all four paths. This makes it possible to show everything in one normalized graphic. These three scenarios give a full picture of the environmental benefits and costs of the proposed MSW-to-jet fuel pathway from three different angles: direct fossil fuel substitution, different ways to manage waste, and how it fits into the larger picture of sustainable aviation fuel pathways that have been reported in the literature. The subsequent subsections delineate and analyze the outcomes for each scenario, supplemented with the pertinent numbers and tables.

4.1.4.1.1. Scenario 1 – MSW-to-jet fuel vs. conventional fossil jet fuel and energy allocation case

This section presents the results for Scenario 1, outlining the comparative environmental performance of the MSW-to-jet fuel pathway against the conventional case defined in this case.

Table 14. Midpoint assessment to produce 1kg of jet fuel in this project from MSW vs. conventional pathway vs. MSW-to-jet fuel with energy allocation

Impact category	Reference unit	Conventional	MSW-to-Jet fuel	MSW-to-Jet fuel with energy allocation
Fine particulate matter formation	kg $PM_{2.5}$ eq	1.34E-03	-1.37E-02	1.22E-04
Fossil resource scarcity	kg oil eq	1.15	-1.02	2.43E-02
Freshwater ecotoxicity	kg 1,4-DCB	4.55E-03	-0.47	5.26E-02
Freshwater eutrophication	kg P eq	2.83E-05	-4.91E-03	3.54E-05
Global warming	kg CO_2 eq	0.46	0.35	0.12
Human carcinogenic toxicity	kg 1,4-DCB	1.49E-02	-0.61	5.34E-02
Human non-carcinogenic toxicity	kg 1,4-DCB	0.15	-4.60	0.17
Ionizing radiation	kBq Co-60 eq	3.03E-02	-2.89	7.79E-03
Land use	m^2a crop eq	3.35E-03	-2.46E-02	2.17E-03
Marine ecotoxicity	kg 1,4-DCB	8.28E-03	-0.60	6.41E-02
Marine eutrophication	kg N eq	4.43E-06	-2.24E-04	1.59E-06
Mineral resource scarcity	kg Cu eq	8.08E-04	6.69E-03	-5.36E-05
Ozone formation, Human health	kg NO_x eq	1.94E-03	7.93E-03	1.37E-04
Ozone formation, Terrestrial ecosystems	kg NO_x eq	2.06E-03	7.91E-03	1.43E-04
Stratospheric ozone depletion	kg CFC11 eq	9.12E-07	-1.41E-06	8.51E-08
Terrestrial acidification	kg SO_2 eq	3.99E-03	2.13E-05	2.36E-04
Terrestrial ecotoxicity	kg 1,4-DCB	1.51	-2.47	0.43
Water consumption	m^3	4.12E-04	-621.76	97.61

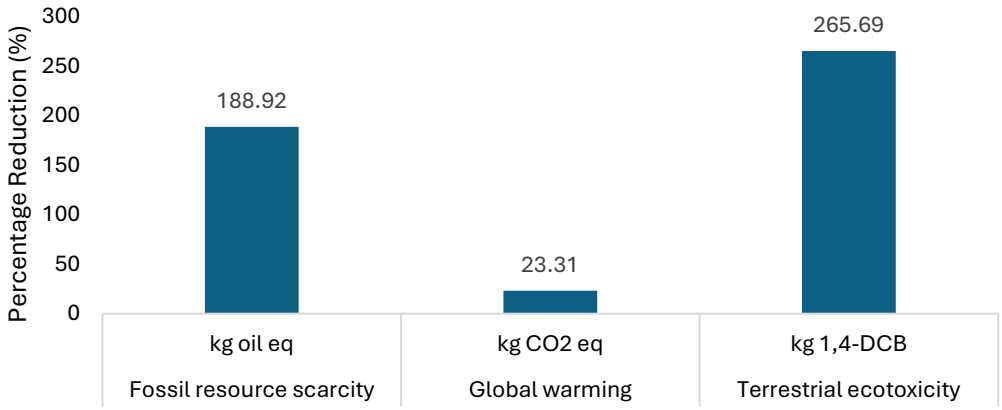

Figure 11. Comparison of percentage reduction in the top 3 impactful midpoint categories

Figure 11 shows how much the proposed MSW-to-jet fuel process reduces the environmental impact in three important areas: terrestrial ecotoxicity, global warming potential, and fossil resource scarcity. The comparison is based on 1 kg of jet fuel for both scenarios. The analysis uses the most recent midpoint LCA results in Table 14, which show that the MSW-derived jet fuel pathway is far better for the environment than the traditional petroleum route. The approach specifically shows that it reduces terrestrial ecotoxicity by about 265%, the potential for global warming by 23%, and the effects of fossil resource scarcity by 189% compared to traditional production.

The main reasons for these improvements are that the feedstock has less of an influence upstream and that resource-intensive operations are replaced with co-product creation. In the MSW-to-jet fuel pathway, OpenLCA models municipal solid waste as a waste item without giving it any environmental credits for its use. However, because it is not associated with the extensive upstream burdens of petroleum feedstocks—such as crude oil extraction, refining, and distribution—it inherently carries much lower baseline impacts. The significant reductions in categories like terrestrial ecotoxicity and fossil resource scarcity are further amplified by the inclusion of avoided product credits for co-products such as diesel, naphtha, light hydrocarbons, and CO_2 utilization, which offset impacts from conventional production routes. Because of this, the MSW pathway gets a lot of net advantages even when there are no credits given to the waste feedstock itself. Overall, this analysis makes it obvious that turning MSW into jet fuel is better for the environment than making jet fuel from fossil fuels. Using a low-burden feedstock, recovering co-products, and replacing high-impact conventional products all work together to lower many important midpoint categories. These results show that waste-based fuels could have a big positive effect on the environment, especially when compared to jet fuel made from petroleum, which has a lot of negative effects on extraction, refining, and distribution.

In addition to the midpoint comparison of chosen categories (such as Global Warming) to the usual approach, a comparable study was done at the endpoint level. In this case, the aggregated

contributions of Global Warming were examined separately within the Human Health and Ecosystem Quality damage categories. This additional comparison provides a higher-level view of how climate-related impacts translate into endpoint burdens. The full results of this extended analysis are included in the Supplementary Data Section (A.1).

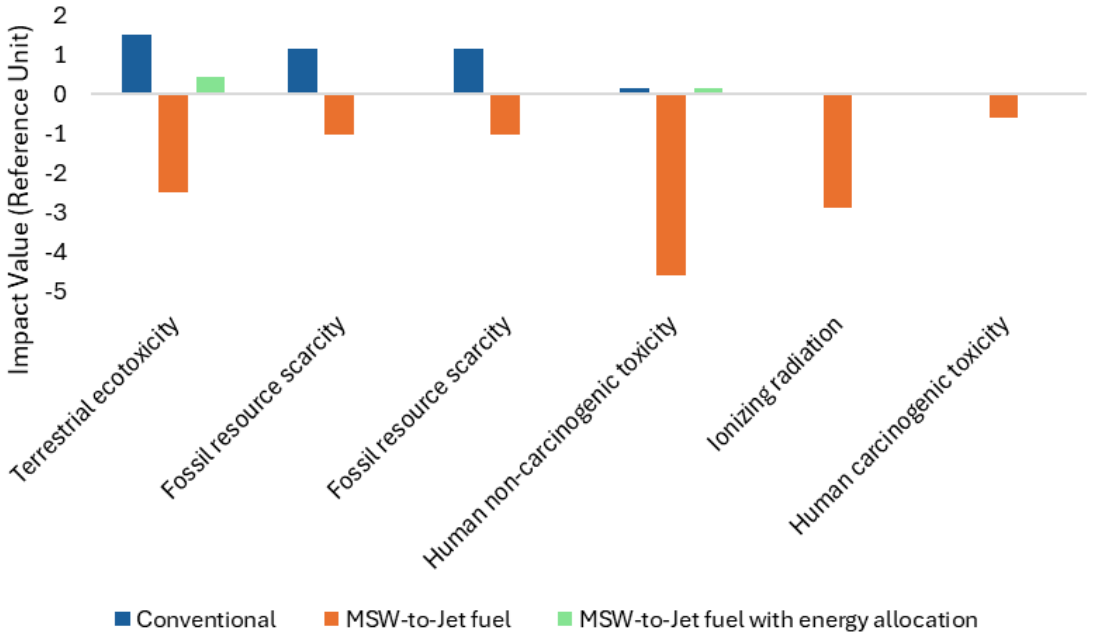

Figure 12. Comparison of Top Six Midpoint Impact Categories by Contribution – Conventional vs. MSW-to-Jet Fuel vs. MSW-to-Jet Fuel with Energy Allocation

Figure 12 shows how the six most important midpoint categories affect the environment in three different cases: the normal fossil-based jet fuel pathway, the MSW-to-jet fuel pathway (which includes avoided products), and the energy allocation approach used in the MSW-to-jet fuel scenario. We chose these groups because they made the biggest difference to the total environmental load. The MSW-to-jet fuel pathway shows big drops in most categories compared to the traditional approach. This is mostly because fossil fuel extraction and the procedures that go along with it are no longer needed. For instance, the amount of ecotoxicity in the ecosystem goes down from 1.51 kg 1,4-DCB eq in the conventional pathway to −2.47 kg 1,4-DCB eq in the MSW scenario. This shows that the environment is better off overall. The same thing happens with fossil resource scarcity, which goes from 1.15 kg oil eq to −1.02 kg oil eq. This shows that the feedstock is renewable. The energy allocation approach, on the other hand, only gives jet fuel a small part of the environmental burden based on how much energy it produces overall. This means that the numbers are less (for example, 0.43 kg 1,4-DCB eq for terrestrial ecotoxicity and 0.024 kg oil eq for fossil resource scarcity).

The disparities between the MSW-to-jet fuel and energy allocation results show how the choices made about distributing the load affect LCA methods. The avoided product approach takes into account the benefits of the whole system by giving co-products credit for replacing traditional manufacturing. On the other hand, energy allocation only looks at jet fuel's proportional contribution, which leads to more conservative (and sometimes positive) results. Along with the midpoint-level analysis, a sensitivity check was also done at the endpoint level to get a clearer idea of how each co-product fits into the picture. In this method, each co-product (diesel, naphtha, light hydrocarbons, and CO_2) was left out of getting avoided product credits one at a time, and the changes in environmental performance that happened as a result were examined. This step-by-step exclusion shows how important each co-product is to the overall net benefits of the MSW pathway. The Supplementary Data Section (A.2) has further information on the results of this analysis, such as graphs and numerical comparisons.

4.1.4.1.2. Scenario 2 – MSW-to-jet fuel vs. MSW incineration for electricity generation

Scenario 2 evaluates the environmental trade-offs of converting MSW into jet fuel compared to its incineration with energy recovery, providing insight into the potential benefits and drawbacks of each utilization pathway.

Table 15. Midpoint assessment to produce MJ of jet fuel and electricity from 1kg of MSW

Impact category	Reference unit	MSW-to-Jet fuel	Conventional
Fine particulate matter formation	kg $PM_{2.5}$ eq	-1.04E-03	1.17E-03
Global warming	kg CO_2 eq	1.37E-03	0.66
Terrestrial acidification	kg SO_2 eq	-6.58E-05	4.04E-03

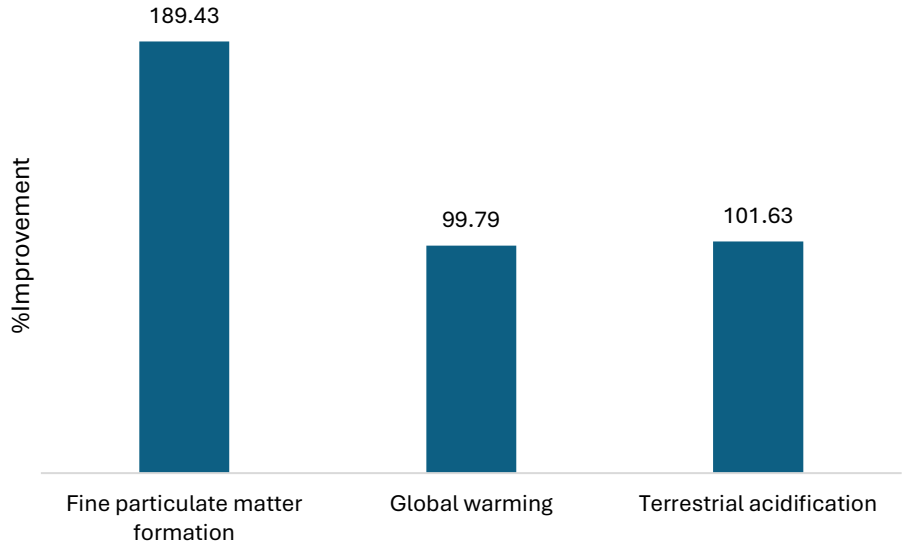

Figure 13. Percentage of improvement in MSW-jet fuel vs. incineration

Figure 13 and Table 15 present a comparative midpoint environmental assessment for the production of 1 MJ of jet fuel via the proposed municipal solid waste MSW-to-jet fuel pathway versus the generation of 1 MJ of electricity through conventional MSW incineration, both scenarios normalized to the same functional input of 1 kg of MSW. Three midpoint impact categories are considered: fine particulate matter formation (kg $PM_{2.5}$ eq), global warming potential (kg CO_2 eq), and terrestrial acidification (kg SO_2 eq).

The MSW-to-jet fuel pathway produces -1.04×10^{-3} kg $PM_{2.5}$ eq of fine particulate matter, while incineration produces 1.17×10^{-3} kg $PM_{2.5}$ eq, which is around 189% better. The MSW-to-jet fuel process also has a big benefit for global warming potential, cutting it by about 100% compared to incineration. Terrestrial acidification also has a good effect, with the approach attaining -6.58×10^{-5} kg SO_2 eq compared to 4.04×10^{-3} kg SO_2 eq for incineration. This means that the pathway avoids a net load. These benefits are mostly due to the fact that co-products like diesel, naphtha, and light hydrocarbons don't have to be burned, and less reliance on fossil-derived inputs. Overall, the results show that the proposed MSW-to-jet fuel pathway routinely beats traditional incineration in all three areas. In fact, it not only reduces but often reverses environmental impacts. The negative numbers seen for fine particulate matter creation and terrestrial acidification are especially interesting since they mean that the process creates net environmental credits, which is not something that happens often with traditional waste treatment methods.

4.1.4.1.3. Scenario 3 – MSW-to-jet fuel vs. literature-based bio jet fuel pathways

In Scenario 3, the analysis examines the performance of the MSW-to-jet fuel pathway in relation to a biojet fuel alternative, offering a comparison that focuses on renewable-based aviation fuels.

Table 16. Comparison of midpoint life cycle impact category results for the MSW-to-jet fuel pathway and selected biojet fuel pathways from the literature

Impact category	**Reference unit**	**MSW-to-Jet Fuel**	**Waste cooking oil**	**Soybean**	**Palm**
Fine particulate matter formation	kg $PM_{2.5}$ eq	-1.47E-02	6.56E-06	1.16E-04	4.50E-06
Fossil resource scarcity	kg oil eq	-0.98	0.02431	0.213	0.00702
Freshwater ecotoxicity	kg 1,4-DCB	-0.38	5.27E-07	0.000142	7.67E-06
Freshwater eutrophication	kg P eq	-4.86E-03	1.16E-06	5.59E-05	1.66E-06
Global warming	kg CO_2 eq	-0.45	2.94E-02	0.391	1.81E-02
Human carcinogenic toxicity	kg 1,4-DCB	-0.52	1.98E-06	9.33E-05	4.80E-06
Human non-carcinogenic toxicity	kg 1,4-DCB	-4.39	1.39E-05	0.0229	1.03E-04
Ionizing radiation	kBq Co-60 eq	-2.86	2.26E-07	4.20E-06	1.20E-07
Land use	m^2a crop eq	-2.07E-02	1.83E-03	7.57E-02	1.61E-03
Marine ecotoxicity	kg 1,4-DCB	-0.48	6.42E-07	5.11E-05	1.43E-06
Marine eutrophication	kg N eq	-2.50E-04	1.63E-04	3.88E-05	5.24E-07
Mineral resource scarcity	kg Cu eq	4.70E-03	4.04E-05	1.18E-03	5.58E-05
Ozone formation, Human health	kg NO_x eq	4.71E-03	3.59E-05	7.63E-04	2.87E-05
Ozone formation, Terrestrial ecosystems	kg NO_x eq	4.69E-03	3.62E-05	7.68E-04	2.90E-05
Stratospheric ozone depletion	kg CFC11 eq	-1.25E-06	1.36E-08	3.77E-07	2.18E-08
Terrestrial acidification	kg SO_2 eq	-3.85E-03	7.00E-05	2.23E-03	1.53E-04
Terrestrial ecotoxicity	kg 1,4-DCB	-2.42	5.70E-04	7.90E-02	2.21E-03
Water consumption	m^3	-455.05	1.73E-04	7.80E-03	1.96E-04

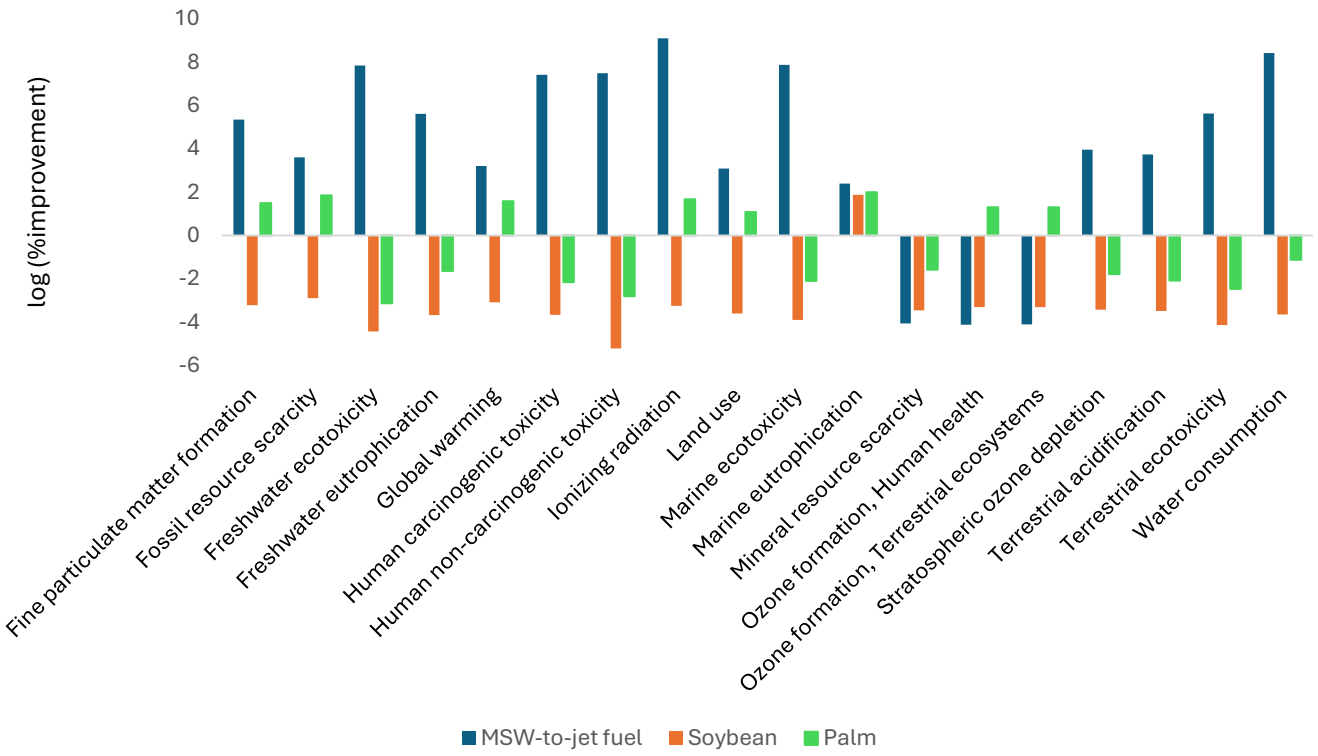

Figure 14. Relative Midpoint Impact Improvements of MSW-to-Jet Fuel, Soybean, and Palm Pathways Compared to Waste Cooking Oil

In this case, the goal is to compare the results of the MSW-to-jet fuel pathway created in this study with biojet fuel paths found in recent research. Both datasets are displayed with a functional unit of 1 MJ of jet fuel produced, facilitating a direct comparison of environmental performance among various production pathways. The literature values are sourced from D'Ascenzo et al. (2022)[36], which conducted a comparative life cycle assessment of several biojet fuel production routes derived from different biomass feedstocks, including waste cooking oil (WCO), soybean, and palm oil. These feedstocks span a range of technological and geographical contexts, from waste-derived to crop-based systems, each with distinct environmental trade-offs.

Figure 14 compares the midpoint life cycle effect categories of three jet fuel pathways—MSW-to-jet fuel, soybean-based jet fuel, and palm-based jet fuel, against waste cooking oil (WCO), which acts as the baseline. The results are shown as percentage improvements on a logarithmic scale. This means that positive values mean less impact compared to WCO, while negative values mean more burden. The literature cases for soybean- and palm-based SAF follow the HEFA route (Hydrotreated Esters & Fatty Acids): refined vegetable oil is pretreated (degumming/bleaching), then hydrotreated and hydro-isomerized with H_2 to remove oxygen as H_2O and to produce a kerosene-range paraffinic product, with naphtha and propane as co-products (allocation in the source study is energy-based). The upstream stage dominates their impacts: for soybean, field

operations (diesel) and fertilizer-related N_2O emissions drive climate, eutrophication and toxicity; for palm, plantation burdens plus POME (palm-oil-mill effluent) management are the main contributors unless biogas capture is applied. In contrast, waste-cooking-oil (WCO) HEFA treats the feedstock as a zero-burden waste, so only collection/cleaning and the HEFA hydrogen demand show up strongly. The MSW→jet case treats MSW as zero-burden at the gate and converts it via gasification and FT, with CO_2 utilization (RWGS) used to tune the H_2/CO ratio. The conversion stage is more energy/H_2-intensive, but Quebec's low-carbon electricity mitigates this, and co-products (diesel, naphtha, light ends) are handled per your model. These different feedstock realities explain the results: MSW-to-jet generally outperforms crop-based HEFA in most midpoint categories (no farming/land-use burdens), is competitive with WCO-HEFA, and shows trade-offs mainly where mineral use (catalysts/alloys, plant materials) or ozone formation (purge-gas NO_x) become influential.

Most categories exhibit big progress on the MSW pathway all the time. For instance, the MSW process reduces fine particulate matter generation by a lot: $–1.47\times10^{-2}$ kg $PM_{2.5}$ eq, while the WCO process only reduces it by $+6.56\times10^{-6}$ kg $PM_{2.5}$ eq. This is the biggest improvement of all the paths. In the same way, MSW shows $–4.86\times10^{-3}$ kg P eq for freshwater eutrophication, while WCO shows $+1.16\times10^{-6}$, which shows a huge averted burden. These avoided effects are most clear in areas that have to do with human toxicity: MSW gets a score of -0.52 kg 1,4-DCB for human carcinogenic toxicity, while WCO gets a score of $+1.98\times10^{-6}$, which is a huge improvement of several orders of magnitude.

In most categories, the soybean and palm routes do worse than WCO. The negative bars show that they have a bigger impact on the environment. For example, soybean-based jet fuel reports +0.213 kg oil eq for fossil resource scarcity, but MSW reports –0.98 kg oil eq. This clearly shows that the waste pathway is better at using resources without fossil fuels. Palm jet fuel also does poorly in terms of land use, with a crop equivalent of +1.61 m^2a, while MSW has $–2.07\times10^{-2}$.

Some categories have more complicated findings. For ozone generation (human health and terrestrial ecosystems), MSW has minor positive values (4.7×10^{-3} kg NO_x eq), which means it has a small effect instead of a big one. However, these values are still significantly lower than those for soybean ($+7.63\times10^{-4}$) or palm ($+2.9\times10^{-5}$). When mineral resources are few, the MSW pathway is worse than WCO ($+4.04\times10^{-5}$ kg Cu eq) because it has a somewhat greater burden of $+4.7\times10^{-3}$. This means that the stages for treating and upgrading waste-derived fuels need more minerals. The figure shows that MSW-to-jet fuel is the best choice in almost all categories. It is many times better than WCO and much better than crop-based bio jet fuels (soybean and palm). The poor performance of soybeans and palm shows that agricultural feedstocks use a lot of land and resources. This makes the environmental benefits of employing waste-derived inputs even stronger.

4.1.4.2. Endpoint Results

The endpoint assessment evaluates the overall environmental consequences of producing 1 kg of jet fuel via the MSW-based pathway in comparison to the conventional fossil-based production route. Using the ReCiPe Endpoint (H) methodology, results are aggregated into higher-level damage categories, namely human health and ecosystem quality, allowing for a more integrated perspective on the potential impacts. These categories take the cumulative effects of several key indicators and turn them into useful measurements, like Disability-Adjusted Life Years (DALY) for human health and species·yr (loss of species over time) for ecosystem quality.

Table 17. Endpoint categories to produce 1 kg of jet fuel in the project vs. the conventional pathway

Impact category	Reference unit	MSW-to-Jet fuel	Conventional
Fine particulate matter formation	DALY	-8.65E-06	8.44E-07
Global warming, Human health	DALY	3.27E-07	4.26E-07
Human carcinogenic toxicity	DALY	-2.04E-06	4.94E-08
Human non-carcinogenic toxicity	DALY	-1.05E-06	3.47E-08
Ionizing radiation	DALY	-2.45E-08	2.57E-10
Ozone formation, Human health	DALY	7.19E-09	1.76E-09
Stratospheric ozone depletion	DALY	-7.52E-10	4.83E-10
Water consumption, Human health	DALY	-1.39E-03	3.54E-10
Freshwater ecotoxicity	species.yr	-3.30E-10	3.15E-12
Freshwater eutrophication	species.yr	-3.29E-09	1.89E-11
Global warming, Freshwater ecosystems	species.yr	2.69E-14	3.51E-14
Global warming, Terrestrial ecosystems	species.yr	9.85E-10	1.28E-09
Land use	species.yr	-2.18E-10	2.98E-11
Marine ecotoxicity	species.yr	-6.33E-11	8.70E-13
Marine eutrophication	species.yr	-3.79E-13	7.54E-15
Ozone formation, Terrestrial ecosystems	species.yr	1.01E-09	2.66E-10
Terrestrial acidification	species.yr	2.40E-12	8.47E-10
Terrestrial ecotoxicity	species.yr	-2.86E-11	1.72E-11
Water consumption, Aquatic ecosystems	species.yr	-3.80E-10	3.26E-16
Water consumption, Terrestrial ecosystem	species.yr	-8.49E-06	2.62E-12
Fossil resource scarcity	USD2013	-0.17	0.52
Mineral resource scarcity	USD2013	1.54E-03	1.86E-04

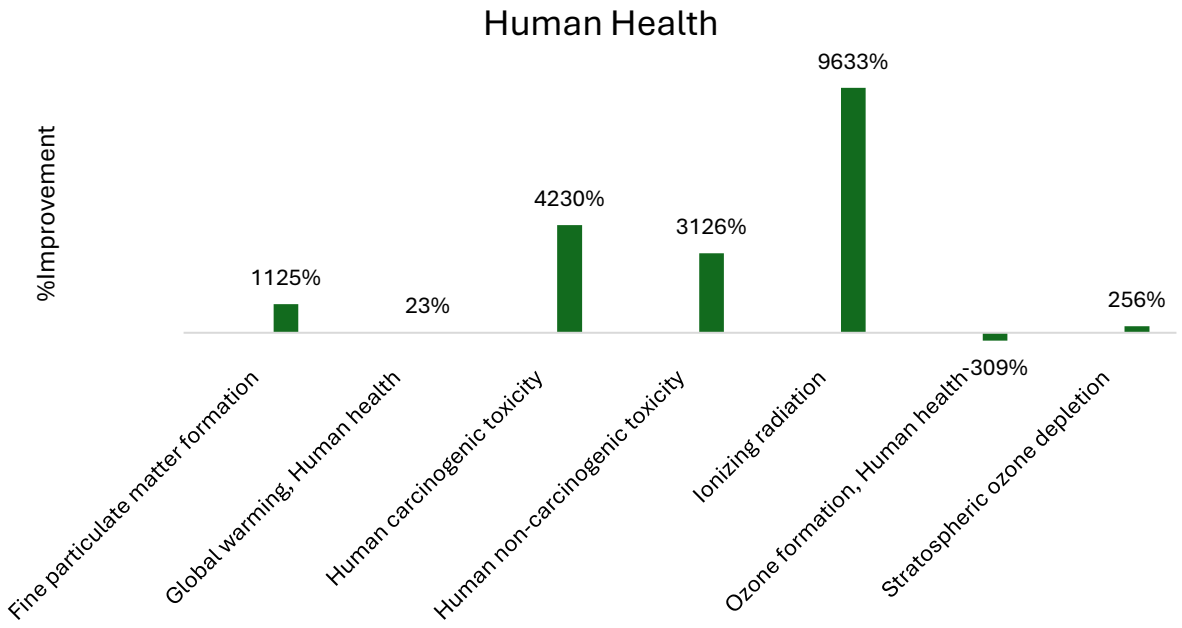

Figure 15. Percentage improvement in human health-related endpoint impact categories for the MSW-to-jet fuel process relative to conventional jet fuel production

Figure 15 compares the percentage improvements in human health–related impacts achieved by the MSW-to-jet fuel pathway over the conventional fossil-based route. In several places, there are a lot of improvements that can be witnessed. For instance, the creation of fine particulate matter improves by more than 1100%, which indicates that health problems linked to it are considerably less likely to happen. The highest decline is in Ionizing Radiation, which has dropped by more than 9600%. There are also great gains in Human Carcinogenic Toxicity (+4230%) and Human Non-Carcinogenic Toxicity (+3126%).

On the other hand, the health effects of climate change (Global Warming, Human Health) are less severe, by 23%, which shows that the benefit is clear but not as strong as in toxicity-related categories. Some impacts are not positive: Ozone Formation, Human Health is going down (–309%), which suggests that there is a trade-off that needs more attention. In general, nevertheless, the MSW-to-jet fuel pathway has quite good health effects in most places.

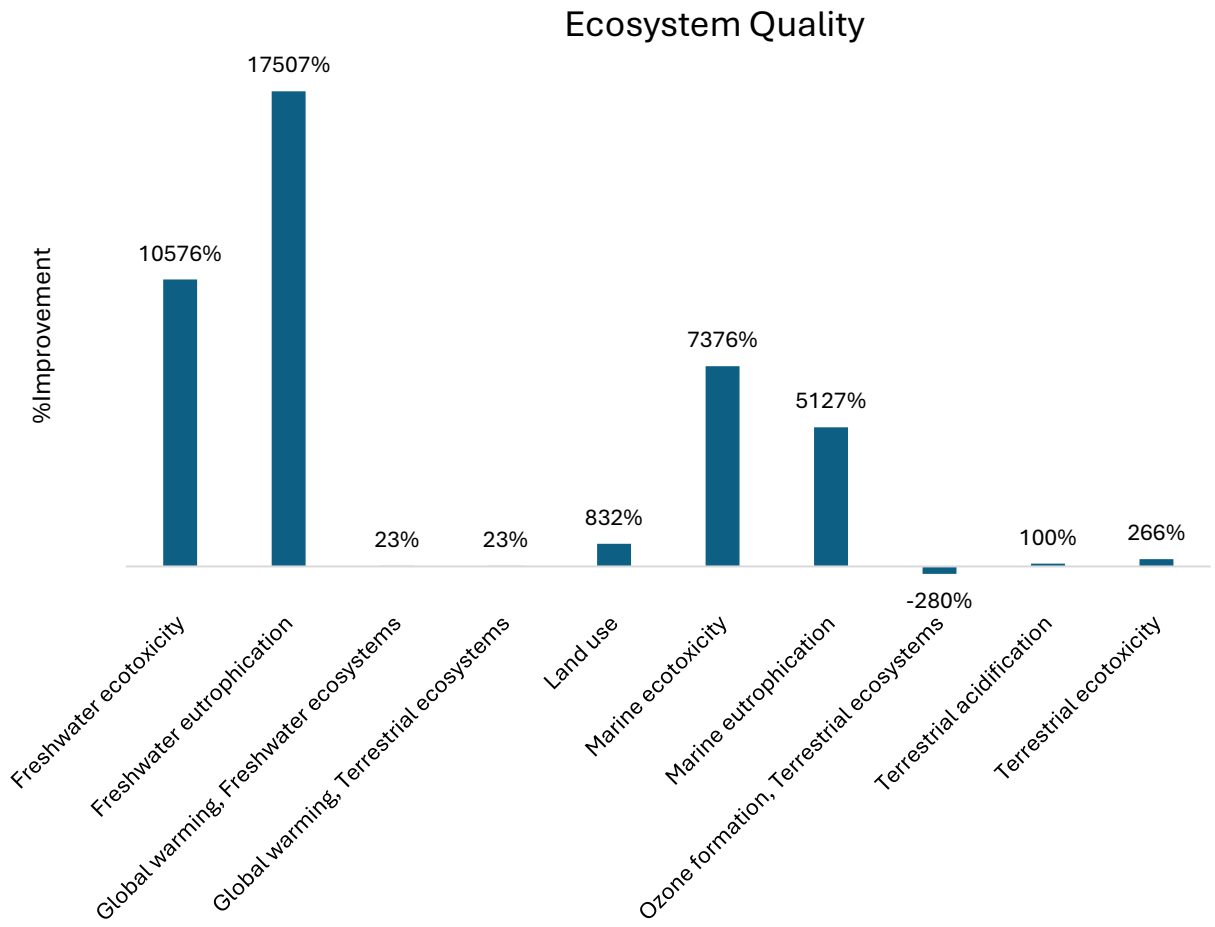

Figure 16. Percentage improvement in ecosystem quality–related endpoint impact categories for the MSW-to-jet fuel process relative to conventional jet fuel production

Figure 16 demonstrates how much better the MSW-to-jet fuel pathway is for ecosystem quality-related impact categories compared to regular fossil-based jet fuel. The results show that there are great environmental benefits in most areas. The most impressive gains are in Freshwater Eutrophication and Freshwater Ecotoxicity, which improve by more than 17,500% and 10,500%, respectively, reflecting the avoidance of nutrient and toxic releases associated with fossil fuel extraction and refining. Marine Ecotoxicity and Marine Eutrophication also reveal large drops in ecological loads, with improvements of more than 7,300% and 5,100%, respectively. Land Use (about 800%) and Terrestrial Ecotoxicity (approximately 266%) both show more moderate but still significant gains. Ecosystem categories connected to global warming improve by roughly 23%.

However, not all impacts are beneficial. Ozone Formation, Terrestrial Ecosystems shows a negative result (–280%), and Terrestrial Acidification shows only a small improvement (~100%). This illustrates that some emissions from the waste conversion pathway can have a bigger effect on these impact categories than the fossil baseline. Still, the general pattern shows that MSW-to-

jet fuel significantly lowers most ecosystem quality harms, which supports its use as a more sustainable option.

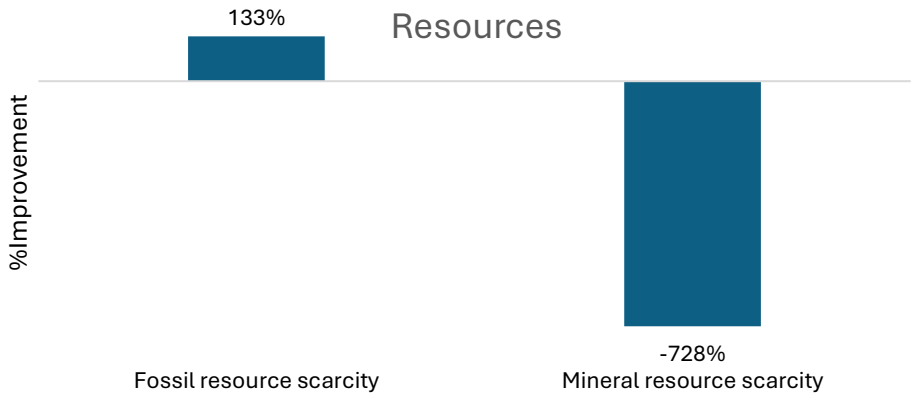

Figure 17. Percentage improvement in resource quality–related endpoint impact categories for the MSW-to-jet fuel process relative to conventional jet fuel production

Figure 17 shows the trade-offs in resource quality effects between the MSW-to-jet fuel pathway and conventional fossil-based jet fuel. The process demonstrates improvement in terms of fossil resource scarcity, with an increase of roughly 133%. This is because employing municipal solid waste as the main feedstock means less reliance on crude oil extraction. The data also suggest a big problem with the lack of mineral resources, with a drop of about 728%. This unfavorable result is mostly due to the upstream needs for catalysts, chemicals, and infrastructure that come with MSW conversion processes, which depend more on minerals. Overall, the approach significantly lessens reliance on fossil resources, but it also creates problems with mineral demand. This shows how important it is to keep coming up with new ideas for catalyst design and process material efficiency to better balance of resources.

4.2. Economic analysis

This section talks about how to find out if the intended way to make jet fuel from MSW is financially sound and competitive. It lists the main assumptions and methodologies used to figure out expenses so that the analysis is transparent and can be done again. We utilize a combination of data from the literature and results from the Aspen Process Economic Analyzer (APEA) to work out how much capital expenditures (CAPEX) will be for big units like the gasification system, syngas treatment, Fischer–Tropsch synthesis, and hydrocracking. These costs include getting equipment, setting it up, and establishing the infrastructure. To gain a whole view of the costs of the process, we look at operating expenses (OPEX), which include items like handling MSW, utilities, maintenance, and labor. To see if the suggested system is financially possible, we look at its net present value (NPV) and expected revenues. We got economic characteristics, market pricing, and cost aspects from books, APEA outputs, and a techno-economic model made in

Microsoft Excel, utilizing methods from Peters, Seider, and other well-known sources. This economic analysis aims to offer valuable insights into the financial feasibility and prospective profitability of the MSW-to-jet fuel pathway, hence advocating for its adoption as a scalable and sustainable solution for waste valorization and low-carbon fuel production.

4.2.1. Assumptions

The economic analysis of the proposed MSW-to-jet fuel production process is built upon assumptions shown in Table 18. A long-term operational view is taken, with set values for the plant's lifetime, building duration, and financial factors like interest rates, debt ratio, and tax rates that are in line with what is normal for chemical process facilities. Current market data and literature are used to set prices for feedstocks, utilities, and products so that cost and revenue estimates are as accurate as possible. Estimating capital costs includes the costs of buying, delivering, and installing major equipment for units like gasification, syngas treatment, Fischer–Tropsch synthesis, and hydrocracking. It also includes the costs of site development, engineering, and start-up to get a complete picture of the investment needs. Operating costs include the costs of managing MSW, utilities, maintenance, and labor. There are set assumptions about workforce levels, overhead, and plant services to show how the process works all the time. These assumptions together make up the basis for figuring out the capital expenditures, operating expenditures, and revenue predictions. This makes sure that the proposed waste-to-jet fuel pathway is evaluated in a clear and methodical fashion from both a technical and economic point of view.

Table 18. Economic analysis parameters, assumptions, and prices

Prices ($US)			
Parameter	**Value**	**Parameter**	**Value**
Base year	2024	**CEPCI[1]**	800.2 (2024)
Electricity	$14.234 per kilowatt of billing demand plus 3.619 cents per kWh [37]		
Labor wage, $/hr	26.26 $/hr [38]	**MSW**	56.8 $/tonne [39]
Kerosene	572 $/tonne [40]	**Diesel**	1369.2 $/tonne [41]
Naphtha	563 $tonne [42]	**Lightend**	500 $/tonne [43]
Liquified CO2	740 $/tonne [44]	**DGA**	2000 $/tonne [45]
Oxygen	66.693 $/tonne [46]	**LPS**	29.29 $/tonne [47]
Process water	1.337 $/tonne [46]	**Hydrogen**	0.869 $/tonne [46]

CAPEX[1] assumptions

Sources used for CAPEX calculation of process units

Gasification: NETL report [27], Gas Treatment: NETL report [27], RWGS: APEA [48] and literature for RWGS reactor [49], FT: APEA [48] and literature for FT reactor [49], Elctrolyzer: NREL report [50]

Parameter	Value	Parameter	Value
Delivery costs	8% of the equipment purchased cost	**Equipment erection**	25% of the equipment delivered cost
Piping	20% of the equipment delivered cost	**Instrumentation and control**	10% of the equipment delivered cost
Electrical	10% of the equipment delivered cost	**Utility cost**	10% of the equipment delivered cost
Off-sites	20% of the equipment delivered cost	**Buildings**	20% of the equipment delivered cost
Site preparation	10% of the equipment delivered cost	**Land**	4% of the equipment delivered cost
Engineering and supervision	15% of the total direct costs	**Construction overhead**	6% of the total direct costs
Project contingency	5% of the fixed capital investment	**Working Capital**	5% of the total capital investment
Start-up costs	8% of the fixed capital investments	**Heat pump installation cost**	20% of equipment cost

OPEX[1] assumptions

Parameter	Value	Parameter	Value
Number of operators per shift	2 (based on 1 process unit)	**Number of shifts**	5
Supervision and engineering	15% of labor wages	**Operating supplies and services**	5% of labor wages
Laboratory expenses	10% of labor wages	**Payroll charges**	30% of total labor wages and supervision
Maintenance wages	3.5% of fixed capital investment (excluding half)	**Maintenance, supervision, and engineering**	25% of maintenance wages
Material supplies	100% of maintenance wages	**Maintenance overhead**	5% of maintenance wages
Plant overhead	7.1% of TWSE[1]	**Mechanical department services**	2.4% of TWSE

Employee relations department	5.9% of TWSE	**Business services**	7.4% of TWSE
Property insurance and taxes, $/yr	2% of fixed capital investment	**Sale expenses**	3% of sales
Research and development	5% of sales	**Administrative expenses**	3% of sales
Economic assumptions			
Parameter	**Value**	**Parameter**	**Value**
Plant lifetime, year	30	**Loan lifetime, year**	15
Capacity factor	90%	**Operation factor**	90%
Construction time, year	3	**Operation time, hr/year**	8760
Loan interest rate	5%	**Federal and provincial tax rate**	26%
Debt ratio	40%	**Internal rate of return**	10%

[1] Abbreviations: CEPCI, chemical engineering plant cost index; CAPEX, capital expenditure; OPEX, operational expenditure; TWSE, total operating and maintenance wages, supervision and engineering expenses.

4.2.2. Capital Cost Estimation

We used both the Aspen Process Economic Analyzer outputs and numbers from the literature for major process units to figure out the capital investment costs. We used APEA for most of the equipment cost estimates. For the Fischer–Tropsch and reverse water–gas shift reactors, we got the costs from Zang et al. (2021) [49]. The cost of the PEM electrolyzer was obtained from data published by the National Renewable Energy Laboratory [50].

Equipment costs were scaled to the desired plant capacity and updated to the base year using the Chemical Engineering Plant Cost Index (CEPCI). The cost of updating was performed using Equation 17:

$$Cost = Cost_{Ref} \times \left(\frac{Capacity}{Capacity_{Ref}}\right)^{n} \times \left(\frac{CEPCI}{CEPCI_{Ref}}\right) \quad (17)$$

Where n is the scaling factor (usually between 0.6 and 1, depending on the type of equipment), this ensures that the capacity and inflation are correctly adjusted to the 2024 CEPCI value utilized in this work. The CAPEX covers the expenses of buying and installing equipment, as well as indirect expenditures like engineering, supervision, and project contingency. This makes sure that the overall fixed capital investment needed for the project is fully reflected. To get the yearly CAPEX, an annualization factor was used on the entire capital investment. This made it possible

to consistently include it to the overall economic model. The annualization factor (AF) was calculated using the equation below:

$$AF = \frac{i(1+i)^N}{(1+i)^N-1} \quad (18)$$

The results of the CAPEX calculations are shown in Table 19.

Table 19. Summary of unit cost and CAPEX

Capital cost of each process unit		
	Gasification	$164,675,650
	Gas treatment	$150,875,861
	Total cost for electrolyser	$303,562,849
	Total installed cost for RWGS	$27,643,991
	Total installed cost for FT	$331,707,469
Working Capital		$45,391,763
Start-up costs		$30,261,176
Total Capital Investment (TCI=Working capital + start-up costs + total cost for gasification, treatment and electrolyser)		$1,073,031,993
Annualized CAPEX		
Interest rate		8.0%
Annualization factor		8.9%
Annualized capital cost, $/yr (= TCI * annualization factor)		$95,314,678

4.2.3. Operating Cost

The costs of running the MSW-to-jet fuel process include the costs of raw materials and utilities needed for continuous operation, as well as fixed costs including labor, maintenance, overhead, property insurance, taxes, and miscellaneous expenses. The pricing of raw materials and utilities came directly from the process simulation outputs in Aspen Plus, which made sure that they matched the system's planned mass and energy balances. We used established methods from Perry's Chemical Engineers' Handbook to figure up labor expenses. These included the size of the facility, the type of operation, the wage rates for workers, the number of shifts, and the number of operators per shift. Maintenance, overhead, and insurance, as examples of continuous costs, were looked at and recognized percentage factors from literature and industry practice were used to make sure we covered all of these costs. Based on the Table 20, the overall yearly operating cost for the proposed process was found to be $162.7 million per year by adding together these parts.

Table 20. Summary of OPEX

Raw Material, $/yr	$32,626,678
Utilities, $/yr	$49,107,591
Operating labour costs (OLC), $/yr	$4,492,561
Maintenance costs (MC), $/yr	$30,450,308
Overhead costs (OHC), $/yr	$4,489,269
Property insurance and taxes, $/yr	$7,565,294
General expenses (GE), $/yr	$33,965,989
Operating costs (OC = raw material + utilities + OLC +MC +MC +OHC +property insurance and tax +GE), $/yr	$162,697,690

4.2.4. Revenue Estimation

To figure out how much revenue the project would make, we looked at the yearly sales of all the main goods made by the system, such as kerosene, diesel, naphtha, light ends, liquefied CO_2, and low-pressure steam. We made sure that the production capabilities and selling prices were in line with current market data so that we could make reasonable revenue estimates. According to Table 21, diesel and kerosene are the biggest sources of total revenue. The sale of liquefied CO_2 and other byproducts comes next, showing that the process produces high-value outputs. The proposed pathway's total annual revenue is expected to be about $308.8 million.

Table 21. Summary of feedstock cost and total revenue

Production Capacity, tonne/hr		70,956
Feedstock		**Cost, $/yr**
	MSW	28,260,187
	Electricity	491,075,901
	Water	41,243
	Oxygen	4,325,219
	DGA	29
Total Cost		81,734,269
Products		**Revenue, $/yr**
	Kerosene	42,572,635
	Diesel	93,294,002
	Naphtha	1,793,877
	Lightend	2,381,821
	Liquified CO_2	148,738,835
	LPS	20,000,549
Total Revenue		**308,781,719**

4.2.6. NPV and MSP

We looked at the net present value (NPV) and the minimum selling price (MSP) of kerosene to see if the proposed MSW-to-jet fuel process would be economically viable. The NPV is the difference between the present value of all the cash inflows and outflows that are predicted to happen over the life of the project, with a certain rate of return (in this case, 10% IRR). A positive NPV means that the project is likely to make more money than it costs to run, which means it is financially sound based on the assumptions made. This analysis assessed NPV throughout a 30-year project life, taking into account revenues from all saleable goods (kerosene, diesel, naphtha, light ends, and liquefied CO_2), as well as capital expenditures, operating expenditures, and any other costs or credits that were relevant. Based on the base-case assumptions and market pricing, the NPV is about $389.78 million, which means that it might be quite profitable.

The MSP is the price at which a product would break even, meaning that the NPV would be zero throughout the course of the project. To put it another way, it's the price needed to pay all of the capital and operating costs at the intended IRR. A high MSP relative to current market prices suggests that the process may not be competitive without subsidies, co-product revenues, or other financial incentives.

To make the MSP calculation consistent with the NPV framework for this multi-product process, a co-product–credited MSP was determined. In this approach, revenues from all co-products except kerosene are credited against the total annualized cost of the plant, and only the remaining cost is allocated to kerosene. The general form of the calculation is:

$$MSP = \frac{TAC - \sum_{i \neq kerosene}(Q_i \times P_i)}{Q_{kerosene}} \quad (19)$$

Where:

- TAC = total annualized cost (annualized CAPEX + OPEX)
- Q_i and P_i = annual quantity and selling price of each co-product
- Q_{ker} = annual kerosene production

This approach reflects the fact that kerosene is produced alongside other valuable products and avoids overstating its required selling price by assuming it must recover all project costs alone. The co-product–credited MSP for kerosene is about $159 per tonne under the base-case conditions. This is a lot lower than the uncredited MSP of about $3,400 per tonne.

This clears up the seeming conflict between the high uncredited MSP and the positive NPV. The uncredited MSP is the price at which costs would be covered if kerosene were the only product responsible for them. The co-product–credited MSP, on the other hand, takes into account the contributions of other products to cost recovery. The credited MSP is a better measure for processes that make a lot of money from co-products, like the MSW-to-jet fuel pathway we looked at here. This study found that the credited MSP of $159 per tonne is much lower than the market jet fuel

price of $572 per tonne. This means that the process could save a lot of money, which would give it a strong competitive edge in the fuel market, especially if it also gets carbon reduction incentives and makes money from selling co-products.

4.2.7. Sensitivity Analysis on MSP

Electricity and MSW prices are the two most volatile and high-leverage cost drivers in this process. Electricity dominates OPEX because many unit operations are power-intensive; MSW fees vary widely by city/contract and can even be negative in some regions or positive (a cost) in others. Stress-testing both shows how much room the project has if power prices spike or if waste contracts change.

In generating the values presented in the sensitivity analysis, all operational and design parameters of the process were maintained at their base-case conditions, including plant capacity, product distribution, energy mix, capital expenditure, and all other input prices. The analysis examines the impact of a singular variable, either the electricity or MSW price, by modifying it by −50%, +50%, and +100% from the baseline value, while maintaining all other parameters constant. The adjusted unit price is used to figure out the yearly operating cost component again. This new cost is then added to the total annual cost of the process. The co-product–credited MSP is subsequently determined following the same methodology as in the base case, whereby revenues from all co-products are subtracted from the total annual cost, and the remaining cost is allocated solely to kerosene production. Since production volumes remain unchanged across scenarios, the variation in MSP is approximately proportional to the change in the tested cost parameter. In cases where the MSP approaches zero, the revenues from co-products are sufficient to cover the entire annual cost, meaning that kerosene could, in theory, be sold at no cost while still achieving breakeven operation.

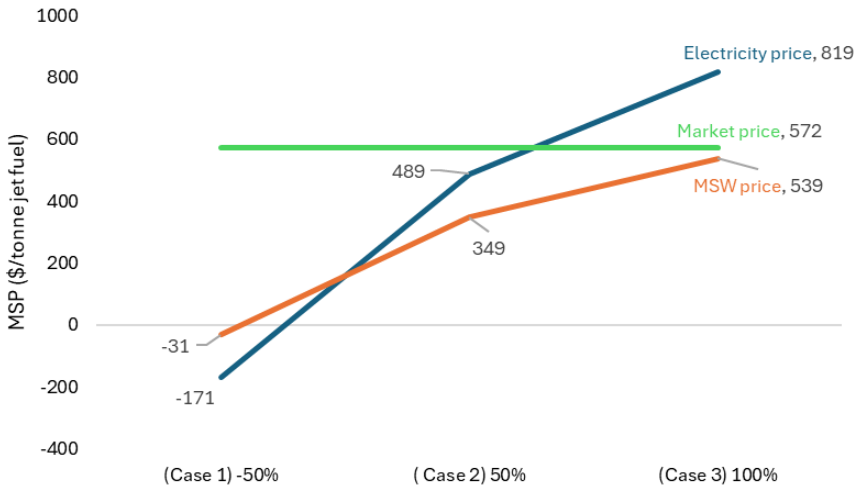

Figure 18. Impact of Electricity and MSW Price Variations on MSP

The graphic above shows how the minimum selling price of jet fuel changes when the costs of electricity and MSW change from the base case of $159 per tonne. Electricity prices are one of the most important factors in economics. When they are doubled, the MSP goes up to over $800 per tonne, which is more than four times higher than the base case. Electricity still has a substantial effect on overall viability, even with a 50% increase. It pushes the MSP to almost 500 $/tonne.

MSW fees also raise the MSP; however, not as much as electricity. If you double the price, the MSP goes up to nearly $540/tonne (about 2.4 times the base scenario). If you only raise it by 50%, the bump is lower. On the other hand, cutting electricity rates in half sends the MSP well into the negative, which shows that when power costs are low, co-product credits more than cover process costs. In practical terms, the project could operate without requiring kerosene revenue under such favorable electricity pricing. MSW reductions have a similar but weaker effect: halving the fee will still substantially lower the need for kerosene-derived revenues, but does not match the impact of electricity reductions.

In general, both inputs have an effect on whether or not a project is profitable, but electricity costs have a much bigger effect on the outcome than MSW fees.

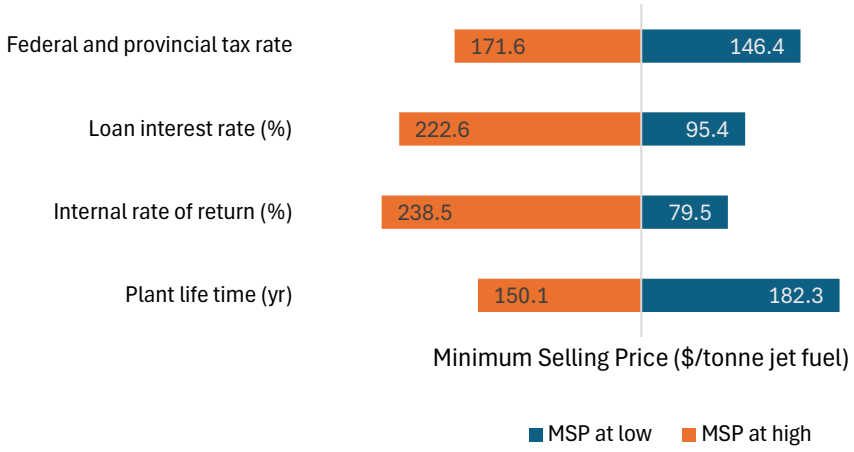

Figure 19. Sensitivity analysis of key financial parameters on the minimum selling price of jet fuel

To evaluate the robustness of the economic performance, another sensitivity analysis was carried out on four key financial parameters: plant lifetime, internal rate of return (IRR), loan interest rate, and federal/provincial tax rate. The base case assumes an MSP of $159/tonne. Each parameter was varied within a reasonable range around its base value, and the resulting MSP was recalculated.

The IRR has the strongest influence. Reducing the IRR to 5% decreases the MSP to $79.5/tonne, while increasing it to 20% raises the MSP to $238.5/tonne. This corresponds to a −50% to +50%

deviation from the base case, showing that investor return expectations nearly triple the selling price range.

The loan interest rate similarly drives major changes in MSP. Lowering the rate to 2% results in an MSP of $95.4/tonne, while raising it to 10% increases the MSP to $222.6/tonne.

The plant lifetime exerts a moderate effect. Extending the operational horizon from 20 to 40 years results in a ±15–20% deviation, reflecting how capital recovery assumptions affect unit production cost.

Finally, the federal and provincial tax rate shows the smallest but still relevant effect. Decreasing the tax burden to 10% reduces the MSP to $146.4/tonne, whereas increasing it to 40% raises it to $171.6/tonne, corresponding to about ±8% deviation.

In summary, this sensitivity analysis demonstrates that financial assumptions dominate the MSP outcome. Among them, IRR and loan interest rate have the largest influence, while plant lifetime and tax rate have more moderate but still noteworthy impacts.

Chapter 5- Conclusion

In this research, we developed an integrated system for the conversion of MSW to jet fuel and other transportation fuels by incorporating CO_2 utilization, with the aim of producing sustainable aviation fuel with reduced environmental impacts and competitive economics. The proposed process tackles the environmental impacts of the aviation and heavy-trucking sectors, two sectors where deep electrification remains impractical because of high energy-density needs. The process design integrated gasification, syngas treatment, reverse water–gas shift, Fischer–Tropsch synthesis, hydrocracking, and product fractionation, supported by Aspen Plus® simulations, Aspen Process Economic Analyzer costing, and OpenLCA for impact assessment. A key strategic choice was to use MSW as a zero-burden, non-food feedstock and to target an FT middle-distillate slate (jet and diesel). Jet fuel was prioritized because it can be a drop-in product with immediate use pathways and it directly addresses a hard-to-abate demand segment in Québec/Canada, and typically enjoys stronger price/credit signals than lower-value cuts. Also, it is based on the fact that IATA mentioned 30% of conventional jet fuel usage should be replaced by bio jet fuels by 2030. Diesel was retained as a co-product because Québec's on-road and off-road markets remain significant, allowing efficient carbon monetization of the FT slate while maintaining drop-in compatibility. Québec is a particularly suitable context for this pathway: its low-carbon, low-cost hydropower enables the additional electricity and hydrogen demands of CO_2 utilization without erasing environmental gains or economic viability, and MSW is available locally at scale.

The techno-economic analysis indicated that, under Québec's electricity pricing, the proposed MSW-to-jet process can achieve a minimum selling price in the competitive range for emerging SAF technologies. The total capital investment for the base case was ~USD 1.07 billion, with operating costs driven mainly by feedstock procurement and electricity consumption. When all co-products were credited against production costs, the base case achieved an MSP of USD 159 per tonne of jet fuel. Sensitivity analyses confirmed that electricity price and MSW price exert the greatest influence on MSP; variations followed near-linear trends when either parameter was adjusted. Importantly, while CCU typically raises OPEX in many regions, in this study the combination of Québec's clean/cheap power, process heat integration, and substantial co-product revenues (diesel, naphtha, light end) offsets those costs, keeping MSP near market parity in plausible ranges. From an economic logic standpoint, prioritizing jet and diesel maximizes value capture from the FT slate (higher unit value and policy support relative to, e.g., power export or single-product routes) and reduces revenue volatility through multi-product offtakes; our sensitivity results also show that co-product credits meaningfully stabilize MSP under electricity/MSW price swings.

The life-cycle assessment benchmarked the base case against three scenarios: (1) conventional fossil-derived jet fuel and an energy-allocation variant of our process, (2) MSW incineration with energy recovery, and (3) literature bio-jet pathways (HEFA from soybean and palm, and WCO). In Scenario 1, the MSW-to-jet route reduced global warming potential by ~23% relative to fossil

jet and substantially lowered fossil resource scarcity and terrestrial ecotoxicity. With full system credits (co-products plus CO_2 utilization), the pathway became net carbon-negative, illustrating the decarbonization leverage of combining waste diversion with CCU in a clean-power context. From an environmental logic perspective, selecting jet and diesel as the primary products delivers large avoided burdens because these middle-distillates displace energy- and emissions-intensive petroleum operations and, unlike electricity from incineration, directly decarbonize end-uses that lack near-term electrification alternatives. Relative to crop-based HEFA (soybean, palm), our route avoids farming, fertilizer use, and land-use change, the main drivers of those pathways, while delivering stronger improvements in human-toxicity and particulate categories; relative to WCO-HEFA, it provides larger potential scale with similar or better performance in most midpoints. The main trade-off observed is mineral resource scarcity, reflecting catalyst and alloy demand, an optimization target for future work (e.g., catalyst life/recycling and deeper electrification/heat-integration to reduce metal-intensive equipment).

Overall, the results show that producing jet fuel (with diesel co-product) from MSW via integrated CO_2 utilization can outperform conventional disposal options and several literature bio-jet routes on both environmental and economic grounds, particularly in jurisdictions like Québec with low-carbon electricity and supportive waste policy. The pathway converts a local liability into certified aviation fuel while co-producing valuable distillates, offering a credible route to near-term SAF supply. By leveraging zero-burden feedstock, co-product valorization, and a clean grid, the design closes the usual affordability gap associated with CCU and positions MSW-to-jet as a scalable, policy-aligned option for deep aviation decarbonization, with the choice of jet and diesel specifically justified by both their higher displacement benefits in LCA and their stronger market/credit economics in this context.

5.1. Future Work

This study offers a thorough assessment of the proposed MSW-to-jet fuel process; yet, numerous opportunities for more research persist. First, process optimization may focus on making energy integration and heat recovery better across the plant. This would lower operating costs and make the operation better for the environment. Second, using renewable electricity sources for electrolysis and other units that use a lot of energy might help the carbon footprint even more and make the system less dependent on fossil fuels. Third, adding more impact categories to the LCA, such as water consumption, land use, and biodiversity impacts, would make the sustainability evaluation more complete.

From an economic standpoint, additional research could investigate alternative financing frameworks, policy incentives (such as low-carbon fuel credits), and fluctuations in co-product markets to evaluate their impact on project feasibility. Lastly, pilot or demonstration-scale deployment would assist in confirming the model's assumptions, improve the parameters for

scaling up, and give real-world operational data for better techno-economic and environmental forecasts.

As another future work, the FT-derived jet cut can be validated against the full ASTM jet-fuel suite, beyond D86, covering density and net heat of combustion, freeze point, kinematic viscosity, total/aromatic content and etc. If the neat paraffinic product is off-spec, tuning and blending with conventional jet fuel can be considered instead of using the product as drop-in to meet the standards.

Supplementary data

A. LCA Results

A.1. Comparison of global warming categories in endpoint results

Figure 20 presents a breakdown of the endpoint results for global warming, showing the relative impact shares on human health and ecosystem quality when comparing the project to the conventional pathway.

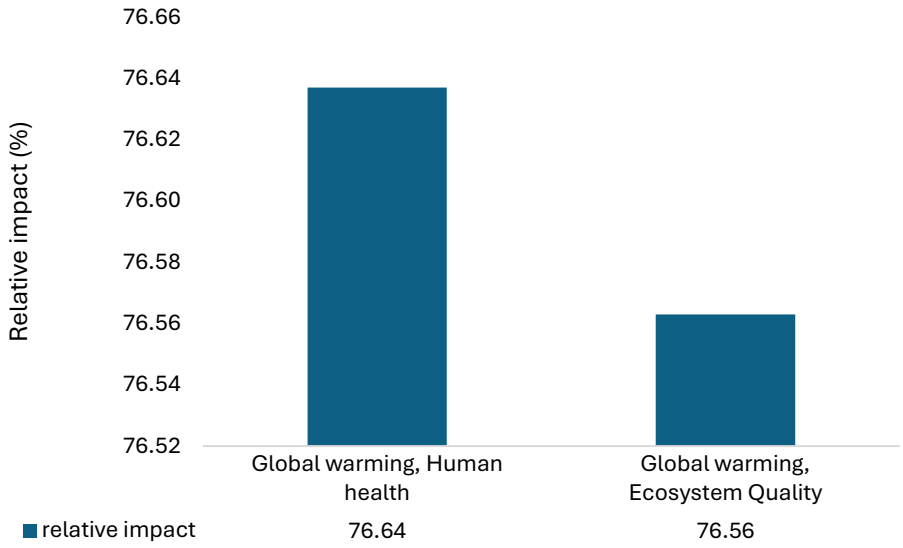

Figure 20. Relative Impact Comparison for Global Warming Categories (Project vs. Conventional Pathway)

The results from the midpoint categories were turned into normalized points so that it would be easier to compare the effects of global warming on human health and ecosystem quality. This method lets you combine categories with different units into a single measure while still being able to compare scenarios. To get a full picture of how global warming affects ecosystem health, the results from freshwater ecosystems and terrestrial ecosystems were added together. The comparison research indicates that the proposed project's impact on global warming (per 1 kg of jet fuel) is roughly 23% lower than that of the conventional method, affecting both human health and ecosystem quality.

A.2. Contribution of co-product on endpoint results

Figure 21presents the relative influence of different co-products on the overall endpoint results, highlighting how excluding each co-product credit individually alters the outcomes.

Table 22. Base Case and Contribution of Individual Co-Products to Selected Endpoint Impact Categories

	Base Case	Diesel Contribution	Naphtha Contribution	Lightend Contribution	CO2 Contribution
Fine particulate matter formation	-8.65E-06	6.89e-07	1.42e-06	7.40e-07	6.66e-07
Fossil resource scarcity	-0.17358	-0.01764	-0.0366	-0.01895	-0.01707
Freshwater ecotoxicity	-3.30E-10	-7.49E-11	-1.55E-10	-8.05E-11	-7.25E-11
Freshwater eutrophication	-3.29E-09	-4.40E-11	-9.13E-11	-4.73E-11	-4.26E-11
Global warming, Freshwater ecosystems	2.69e-14	7.10e-14	1.47e-13	7.63e-14	6.87e-14
Global warming, Human health	3.27e-07	8.61e-07	1.78e-06	9.25e-07	8.33e-07
Global warming, Terrestrial ecosystems	9.85e-10	2.59e-09	5.39e-09	2.79e-09	2.51e-09
Human carcinogenic toxicity	-2.05E-06	-3.64E-07	-7.55E-07	-3.91E-07	-3.52E-07
Human non-carcinogenic toxicity	-1.05E-06	-5.52E-08	-1.14E-07	-5.93E-08	-5.34E-08
Ionizing radiation	-2.46E-08	-3.04E-10	-6.31E-10	-3.27E-10	-2.94E-10
Land use	-2.19E-10	-3.98E-11	-8.25E-11	-4.27E-11	-3.85E-11
Marine ecotoxicity	-6.34E-11	-1.38E-11	-2.86E-11	-1.49E-11	-1.34E-11
Marine eutrophication	-3.80E-13	5.12e-14	1.06e-13	5.50e-14	4.95e-14
Mineral resource scarcity	0.00155	0.00053	0.0011	0.00057	0.00051

Ozone formation, Human health	7.19e-09	3.36e-09	5.05e-09	3.61e-09	3.25e-09
Ozone formation, Terrestrial ecosystems	1.01e-09	4.77e-10	7.47e-10	5.12e-10	4.61e-10
Stratospheric ozone depletion	-7.53E-10	-9.85E-11	-2.04E-10	-1.06E-10	-9.53E-11
Terrestrial acidification	2.409e-12	1.18e-11	2.19e-11	1.25e-11	1.15e-11
Terrestrial ecotoxicity	-2.86E-11	-1.13E-12	-2.34E-12	-1.21E-12	-1.09E-12
Water consumption, Aquatic ecosystem	-3.80E-10	-1.21E-10	-2.52E-10	-1.30E-10	-1.17E-10
Water consumption, Human health	-0.0014	-0.00045	-0.00093	-0.00048	-0.00043

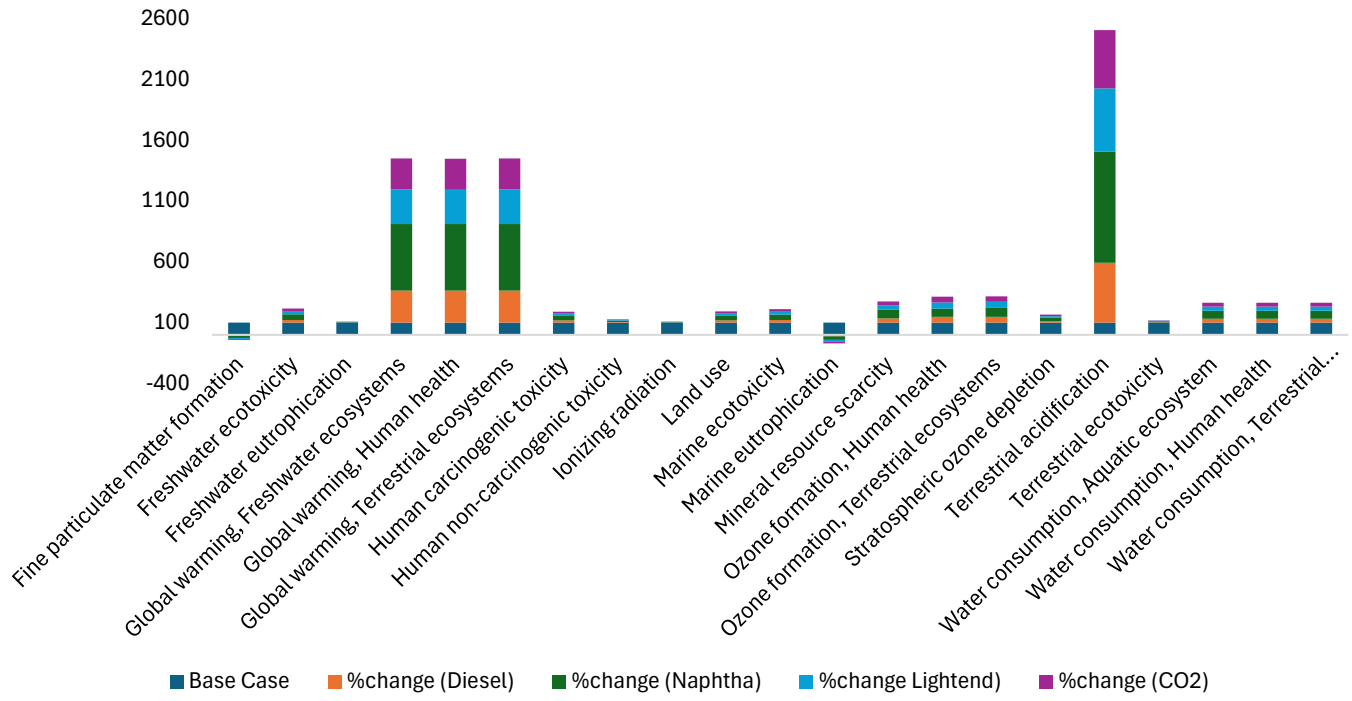

Figure 21. Comparison of the base case LCA results with scenarios excluding individual co-products

Table 22 presents the endpoint impact category results for the base case scenario alongside the calculated contribution of each co-product including diesel, naphtha, light ends, and CO_2 when excluded from the avoided product credits. In the base case, all co-products are treated as avoided products, meaning that their production displaces equivalent market products and thus brings environmental credits. This often results in negative values for certain categories, such as Fine particulate matter formation ($–8.65 \times 10^{–6}$ DALY) and Fossil resource scarcity (–0.17358 USD2013), indicating an overall environmental benefit. To determine the contribution of each co-product, a scenario was modeled where that specific co-product was not credited as an avoided product. For example, the exclusion of diesel increased Fossil resource scarcity by 0.01764 USD2013, while excluding naphtha increased the same category by 0.0366 USD2013. This method makes it possible to measure how much each co-product contributes to the overall environmental benefits in the base scenario.

Figure 21 shows how much diesel, naphtha, light ends, and CO_2 each contribute to each endpoint effect category, as a percentage of the base case. The base case numbers are set at 100%, while the other bars show how much the percentage changes when each co-product is left out. This column style lets you see right away how much each co-product affects the others. For example, in Global warming and Freshwater ecosystems, taking out naphtha raises the effect to around 547% of the base case value. Light ends and CO_2 raise it by about 284% and 255%, respectively. Terrestrial ecotoxicity also goes up a lot, with the absence of diesel causing it to go up by more than 2000% compared to the basic case. These results show that the negative values in the basic scenario are mostly caused by the avoided product credits from co-products. They also show that some categories are more sensitive to certain co-products than others.

References

[1] N.D. Khuong, N.L. Hoang, S.T. Aleksandrovna, Gasification of municipal solid waste has high moisture content, in: 2021 3rd Int. Youth Conf. Radio Electron. Electr. Power Eng. REEPE, IEEE, Moscow, Russia, 2021: pp. 1–4. https://doi.org/10.1109/reepe51337.2021.9388057.

[2] M.T. Munir, I. Mardon, S. Al-Zuhair, A. Shawabkeh, N.U. Saqib, Plasma gasification of municipal solid waste for waste-to-value processing, Renew. Sustain. Energy Rev. 116 (2019) 109461. https://doi.org/10.1016/j.rser.2019.109461.

[3] M.M. Tun, D. Juchelková, Drying methods for municipal solid waste quality improvement in the developed and developing countries: A review, Environ. Eng. Res. 24 (2018) 529–542. https://doi.org/10.4491/eer.2018.327.

[4] M. Sajid, A. Raheem, N. Ullah, M. Asim, M.S. Ur Rehman, N. Ali, Gasification of municipal solid waste: Progress, challenges, and prospects, Renew. Sustain. Energy Rev. 168 (2022) 112815. https://doi.org/10.1016/j.rser.2022.112815.

[5] S. Kwon, S. Im, Feasibility of non-thermal plasma gasification for a waste-to-energy power plant, Energy Convers. Manag. 251 (2022) 114978. https://doi.org/10.1016/j.enconman.2021.114978.

[6] C. Chen, Y.-Q. Jin, J.-H. Yan, Y. Chi, Simulation of municipal solid waste gasification in two different types of fixed bed reactors, Fuel 103 (2013) 58–63. https://doi.org/10.1016/j.fuel.2011.06.075.

[7] M.P.S. Santos, D.P. Hanak, Techno-economic feasibility assessment of sorption enhanced gasification of municipal solid waste for hydrogen production, Int. J. Hydrog. Energy 47 (2022) 6586–6604. https://doi.org/10.1016/j.ijhydene.2021.12.037.

[8] A.A. Arpia, T.-B. Nguyen, W.-H. Chen, C.-D. Dong, Y.S. Ok, Microwave-assisted gasification of biomass for sustainable and energy-efficient biohydrogen and biosyngas production: A state-of-the-art review, Chemosphere 287 (2022) 132014. https://doi.org/10.1016/j.chemosphere.2021.132014.

[9] T. Kandaramath Hari, Z. Yaakob, N.N. Binitha, Aviation biofuel from renewable resources: Routes, opportunities and challenges, Renew. Sustain. Energy Rev. 42 (2015) 1234–1244. https://doi.org/10.1016/j.rser.2014.10.095.

[10] Aviation Turbine Fuels Through the Fischer–Tropsch Process, in: Biofuels Aviat., Elsevier, 2016: pp. 241–259. https://doi.org/10.1016/b978-0-12-804568-8.00010-x.

[11] A. Laurent, I. Bakas, J. Clavreul, A. Bernstad, M. Niero, E. Gentil, M.Z. Hauschild, T.H. Christensen, Review of LCA studies of solid waste management systems – Part I: Lessons learned and perspectives, Waste Manag. 34 (2014) 573–588. https://doi.org/10.1016/j.wasman.2013.10.045.

[12] IPCC, 2006 IPCC Guidelines for National Greenhouse Gas Inventories: Volume 5 – Waste, Institute for Global Environmental Strategies (IGES), 2006. https://www.ipcc-nggip.iges.or.jp/public/2006gl/vol5.html.

[13] A.S. Ouedraogo, R.S. Frazier, A. Kumar, Comparative Life Cycle Assessment of Gasification and Landfilling for Disposal of Municipal Solid Wastes, Energies 14 (2021) 7032. https://doi.org/10.3390/en14217032.

[14] T. Astrup, J. Møller, T. Fruergaard, Incineration and co-combustion of waste: accounting of greenhouse gases and global warming contributions, Waste Manag. Res. J. Sustain. Circ. Econ. 27 (2009) 789–799. https://doi.org/10.1177/0734242x09343774.

[15] U. Arena, Process and technological aspects of municipal solid waste gasification. A review, Waste Manag. 32 (2012) 625–639. https://doi.org/10.1016/j.wasman.2011.09.025.
[16] D. Fernández-Domínguez, S. Astals, M. Peces, N. Frison, D. Bolzonella, J. Mata-Alvarez, J. Dosta, Volatile fatty acids production from biowaste at mechanical-biological treatment plants: Focusing on fermentation temperature, Sci. Total Environ. 747 (2020).
[17] E. Papadopoulou, C. Vance, P.S.R. Vallespin, I. Angelidaki, Saccharina latissima, candy-factory waste, and digestate from full-scale biogas plant as alternative carbohydrate and nutrient sources for lactic acid production, (n.d.).
[18] L. Yu, M.Y. Khalid, M.M. Ameen, M.S. Hossain, M.T.H. Sultan, M. Bin Khalid, Biofuel production by hydrothermal liquefaction of municipal solid waste: process characterization and optimization, Sci. Rep. 13 (2023).
[19] N. Scarlat, J.-F. Dallemand, F. Fahl, Biogas: Developments and perspectives in Europe, Renew. Energy 129 (2018) 457–472. https://doi.org/10.1016/j.renene.2018.03.006.
[20] Z. Liu, H. Liu, X. Yang, Life Cycle Assessment of the Cellulosic Jet Fuel Derived from Agriculture Residue, Aerospace 10 (2023) 129. https://doi.org/10.3390/aerospace10020129.
[21] F. Pierobon, I.L. Eastin, I. Ganguly, Life cycle assessment of residual lignocellulosic biomass-based jet fuel with activated carbon and lignosulfonate as co-products, Biotechnol. Biofuels 11 (2018). https://doi.org/10.1186/s13068-018-1141-9.
[22] J.P. Ahire, R. Bergman, T. Runge, S.H. Mousavi-Avval, D. Bhattacharyya, T. Brown, J. Wang, Techno-economic and environmental impacts assessments of sustainable aviation fuel production from forest residues, Sustain. Energy Fuels 8 (2024) 4602–4616. https://doi.org/10.1039/d4se00749b.
[23] C. Moretti, I. Vera, M. Junginger, A. López-Contreras, L. Shen, Attributional and consequential LCAs of a novel bio-jet fuel from Dutch potato by-products, Sci. Total Environ. 813 (2022) 152505. https://doi.org/10.1016/j.scitotenv.2021.152505.
[24] J. Han, A. Elgowainy, H. Cai, M.Q. Wang, Life-cycle analysis of bio-based aviation fuels, Bioresour. Technol. 150 (2013) 447–456. https://doi.org/10.1016/j.biortech.2013.07.153.
[25] R. Batten, M. Karanjikar, S. Spatari, A sustainable aviation fuel pathway from biomass: life cycle environmental and cost evaluation for dimethylcyclooctane jet fuel, Sustain. Energy Fuels 8 (2024) 1924–1935. https://doi.org/10.1039/d3se01470c.
[26] E. Budsberg, J.T. Crawford, H. Morgan, W.S. Chin, R. Bura, R. Gustafson, Hydrocarbon bio-jet fuel from bioconversion of poplar biomass: life cycle assessment, Biotechnol. Biofuels 9 (2016). https://doi.org/10.1186/s13068-016-0582-2.
[27] U.S. Department of Energy – National Energy Technology Laboratory (NETL), Cost and Performance Baseline for Fossil Energy Plants Volume 1: Bituminous Coal and Natural Gas to Electricity, NETL, Pittsburgh, PA, 2010.
[28] solid waste diversion and disposal per person, (n.d.). https://www.canada.ca/en/environment-climate-change/services/environmental-indicators/solid-waste-diversion-disposal.html (accessed July 15, 2025).
[29] C. Sheng, J.L.T. Azevedo, Estimating the higher heating value of biomass fuels from basic analysis data, Biomass Bioenergy 28 (2005) 499–507. https://doi.org/10.1016/j.biombioe.2004.11.008.
[30] G.P. Van Der Laan, A.A.C.M. Beenackers, Kinetics and Selectivity of the Fischer–Tropsch Synthesis: A Literature Review, Catal. Rev. 41 (1999) 255–318. https://doi.org/10.1081/cr-100101170.

[31] W. Ma, G. Jacobs, D.E. Sparks, R.L. Spicer, B.H. Davis, J.L.S. Klettlinger, C.H. Yen, Fischer–Tropsch synthesis: Kinetics and water effect study over 25%Co/Al2O3 catalysts, Catal. Today 228 (2014) 158–166. https://doi.org/10.1016/j.cattod.2013.10.014.
[32] J. Chang, L. Bai, B. Teng, R. Zhang, J. Yang, Y. Xu, H. Xiang, Y. Li, Kinetic modeling of Fischer–Tropsch synthesis overFe–Cu–K–SiO2catalyst in slurry phase reactor, Chem. Eng. Sci. 62 (2007) 4983–4991. https://doi.org/10.1016/j.ces.2006.12.031.
[33] J. Eilers, S.A. Posthuma, S.T. Sie, The Shell Middle Distillate Synthesis Process (SMDS), Catal. Lett. 7 (1990) 253–269.
[34] U.M. Teles, F.A.N. Fernandes, Hydrocracking of Fischer-Tropsch Products. Optimization of Diesel and Naphtha Cuts, (n.d.).
[35] ASTM International, ASTM D86-17a: Standard Test Method for Distillation of Petroleum Products and Liquid Fuels at Atmospheric Pressure, West Conshohocken, PA, 2017.
[36] F. D'Ascenzo, G. Vinci, M. Savastano, A. Amici, M. Ruggeri, Comparative Life Cycle Assessment of Sustainable Aviation Fuel Production from Different Biomasses, Sustainability 16 (2024) 6875. https://doi.org/10.3390/su16166875.
[37] electricity price, (https://www.hydroquebec.com/data/documents-donnees/pdf/electricity-rates.pdf#page=87). https://www.hydroquebec.com/data/documents-donnees/pdf/electricity-rates.pdf#page=87.
[38] labor wage, (2017). https://www.bls.gov/oes/2017/may/oes_nat.htm#51-0000.
[39] MSW price, (n.d.). https://erefdn.org/analyzing-municipal-solid-waste-landfill-tipping-fees/.
[40] kerosene price, (n.d.). https://www.intratec.us/products/energy-price-references/commodity/kerosene-price-canada.
[41] diesel price, (n.d.). https://kalibrate.com/insights/blog/fuel-pricing/october-2024-kalibrates-canadian-petroleum-price-snapshot.
[42] naphtha price, (2024). https://kalibrate.com/insights/blog/fuel-pricing/october-2024-kalibrates-canadian-petroleum-price-snapshot.
[43] Lightend price, (n.d.). https://www.echemi.com/pip/propane-pid_Rock16615.html.
[44] liquified CO2 price, (n.d.). https://www.openpr.com/news/3790958/liquid-carbon-dioxide-prices-reflect-strong-demand-and-supply.
[45] DGA price, (n.d.). https://qdeverchemical.en.made-in-china.com/product/QxcrFVYEJNhH/China-Professional-Vendor-Diglycolamine-99-CAS-929-06-6.html?pv_id=1j24o2oc6ac1&faw_id=1j24o3c5u070&bv_id=1j24o3un782f.
[46] Methanol Worked Examples for the TEA and LCA Guidelines for CO2 Utilization, Global CO2 Initiative@UM, 2018. https://doi.org/10.3998/2027.42/145723.
[47] LPS price, (n.d.). https://holooly.com/solutions-v2-1/determine-the-cost-of-producing-high-medium-and-low-pressure-steam-using-a-natural-gas-fuel-source-for-medium-and-low-pressure-steam-production-assume-that-steam-is-produced-at-the-highest-pres
[48] Aspen Technology, Inc., Aspen Process Economic Analyzer (APEA), Version 14.0, (2024).
[49] G. Zang, P. Sun, A.A. Elgowainy, A. Bafana, M. Wang, Performance and cost analysis of liquid fuel production from H2 and CO2 based on the Fischer-Tropsch process, J. CO2 Util. 46 (2021) 101459. https://doi.org/10.1016/j.jcou.2021.101459.
[50] A. Badgett, J. Brauch, A. Thatte, R. Rubin, C. Skangos, X. Wang, R. Ahluwalia, B. Pivovar, M. Ruth, Updated Manufactured Cost Analysis for Proton Exchange Membrane Water Electrolyzers, 2024. https://doi.org/10.2172/2311140.